

## V. 研究成果の刊行物・別冊



## Angioimmunoblastic T-cell lymphoma mice model

Fumihiko Sato<sup>a,b</sup>, Takashi Ishida<sup>a,\*</sup>, Asahi Ito<sup>a</sup>, Fumiko Mori<sup>a</sup>, Ayako Masaki<sup>a</sup>, Hisashi Takino<sup>b</sup>, Tomoko Narita<sup>a</sup>, Masaki Ri<sup>a</sup>, Shigeru Kusumoto<sup>a</sup>, Susumu Suzuki<sup>c</sup>, Hirokazu Komatsu<sup>a</sup>, Akio Niimi<sup>a</sup>, Ryuzo Ueda<sup>c</sup>, Hiroshi Inagaki<sup>b</sup>, Shinsuke Iida<sup>a</sup>

<sup>a</sup> Department of Medical Oncology and Immunology, Nagoya City University Graduate School of Medical Sciences, 1 Kawasumi, Mizuho-chou, Mizuho-ku, Nagoya, Aichi 467-8601, Japan

<sup>b</sup> Department of Anatomic Pathology and Molecular Diagnostics, Nagoya City University Graduate School of Medical Sciences, 1 Kawasumi, Mizuho-chou, Mizuho-ku, Nagoya, Aichi 467-8601, Japan

<sup>c</sup> Department of Tumor Immunology, Aichi Medical University School of Medicine, Nagakute, Aichi 480-1195, Japan

### ARTICLE INFO

#### Article history:

Received 7 May 2012

Received in revised form 26 July 2012

Accepted 11 September 2012

Available online 29 September 2012

#### Keywords:

Angioimmunoblastic T-cell lymphoma

Follicular helper T cell

BCL6

PD1

NOG mice

Tumor microenvironment

### ABSTRACT

We established an angioimmunoblastic T-cell lymphoma (AITL) mouse model using NOD/Shi-*scid*, IL-2R $\gamma^{\text{null}}$  mice as recipients. The immunohistological findings of the AITL mice were almost identical to those of patients with AITL. In addition, substantial amounts of human immunoglobulin G/A/M were detected in the sera of the AITL mice. This result indicates that AITL tumor cells helped antibody production by B cells or plasma cells. This is the first report of reconstituting follicular helper T (TFH) function in AITL cells in an experimental model, and this is consistent with the theory that TFH cell is the cell of origin of AITL tumor cells.

© 2012 Elsevier Ltd. All rights reserved.

## 1. Introduction

Angioimmunoblastic T-cell lymphoma (AITL) represents a distinct clinicopathological entity among nodal peripheral T-cell lymphomas. A complex network of interactions between AITL tumor cells and the various reactive cellular components of the tumor microenvironment forms the clinical and histological features of AITL [1]. Because of its complexity, analysis of the immunopathogenesis of AITL *in vitro* seems to be impossible. On the other hand, recent advances in the development of novel mouse models, in which human hematopoietic and/or immune systems could be reconstituted, have contributed to analyzing the pathogenesis of various human diseases and evaluating the effects of therapeutic agents [2–6]. In the present study, we aimed to establish a novel AITL mouse model in which both primary tumor cells of human AITL and microenvironmental reactive cells engraft and interact with each other, using NOD/Shi-*scid*, IL-2R $\gamma^{\text{null}}$  (NOG) mice [7,8] as recipients, and analyzed the immunopathogenesis of AITL.

## 2. Materials and methods

### 2.1. Human cells

The donors of tumor cells provided written informed consent before sampling in accordance with the Declaration of Helsinki. The present study was approved by the institutional ethics committee of Nagoya City University Graduate School of Medical Sciences.

### 2.2. Animals

NOG mice were purchased from the Central Institute for Experimental Animals and used at 6–8 weeks of age. All of the *in vivo* experiments were performed in accordance with the United Kingdom Coordinating Committee on Cancer Research Guidelines for the Welfare of Animals in Experimental Neoplasia, Second Edition, and were approved by the ethics committee of the Center for Experimental Animal Science, Nagoya City University Graduate School of Medical Sciences.

### 2.3. Primary AITL cell-bearing mouse model

The affected lymph node cells from two patients with AITL were suspended in RPMI-1640, and intraperitoneally (i.p.) injected into NOG mice. Lymph node cells of AITL patient 1 were injected at a dose of  $2.5 \times 10^7$  lymph node cells/mouse (total 2 mice), and those of patient 2 were injected at a dose of  $4.0 \times 10^6$  lymph node cells/mouse (total 3 mice). When mice that had received lymph node cells from patient 1 or 2 became weakened, they were sacrificed at day 34 and 48, respectively.

### 2.4. Antibodies and flow cytometry

The following antibodies were used for flow cytometry: MultiTEST CD3 (clone SK7) FITC/CD16 (B73.1)+CD56 (NCAM 16.2) PE/CD45 (2D1) PerCP/CD19 (SJ25C1)

\* Corresponding author. Tel.: +81 52 853 8216; fax: +81 52 852 0849.  
E-mail address: itakashi@med.nagoya-cu.ac.jp (T. Ishida).

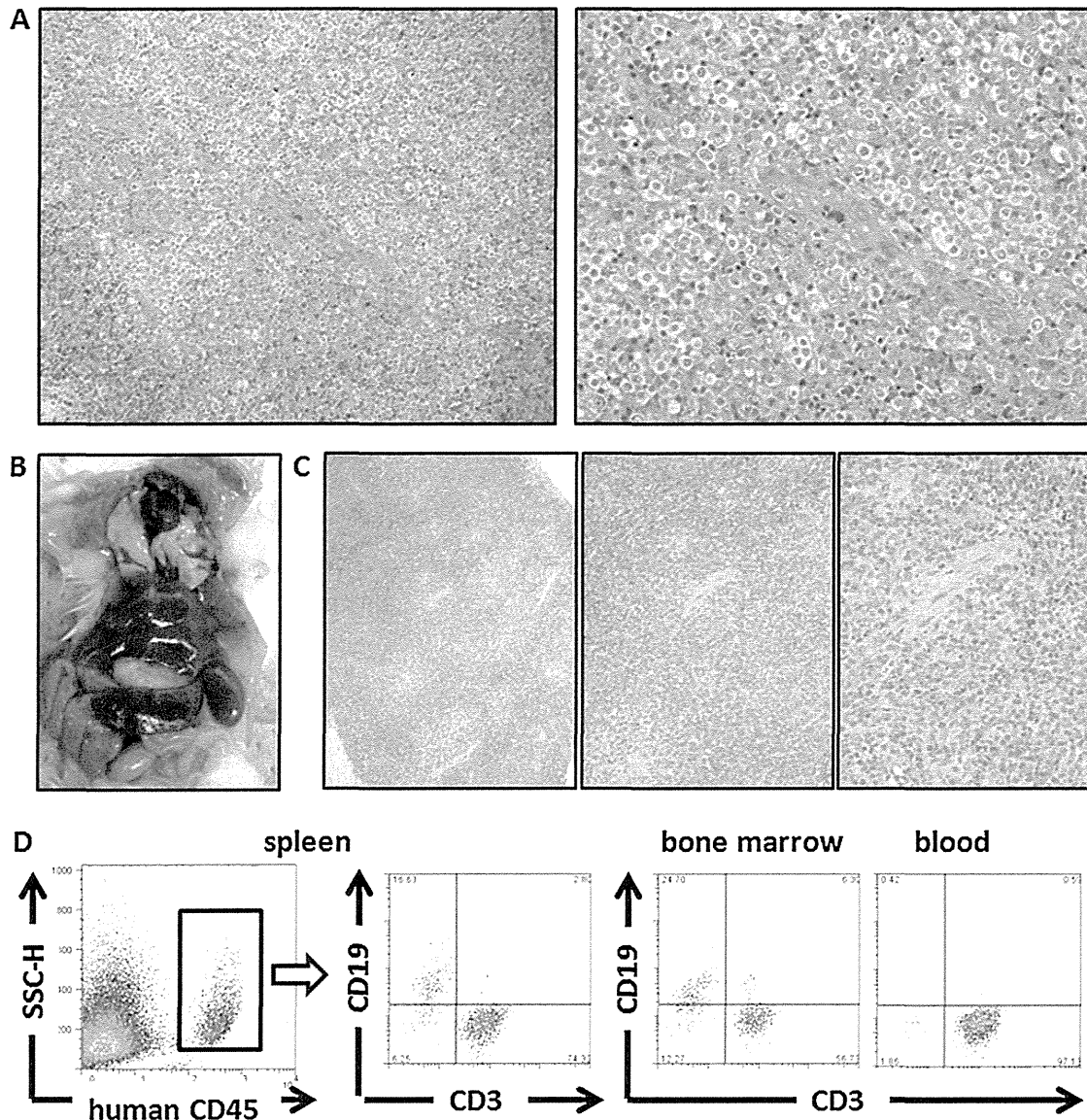


**Fig. 1.** Primary AITL cell-bearing NOG mouse model. (A) Microscopic images with hematoxylin and eosin staining of the affected lymph node of AITL patient 1 are shown. (B) Macroscopic image of a primary AITL cell-bearing NOG mouse is shown. (C) Sections of the AITL-affected mouse spleen with hematoxylin and eosin staining are shown. (D) The presence of human CD45-positive cells in the infiltrate of the mouse spleen, bone marrow, and blood was determined by flow cytometric analysis of human CD3 and CD19 expression.

APC Reagent, MultiTEST CD3 FITC/CD8 (SK1) PE/CD45 PerCP/CD4 (SK3) APC Reagent. All antibodies were purchased from BD Biosciences (San Jose, CA, USA). Whole blood cells from mice were treated with BD FACS lysing solution (BD Biosciences) for lysing red blood cells. Cells were analyzed by a FACSCalibur (BD Biosciences) with the aid of FlowJo software (Tree Star, Inc., Ashland, OR, USA).

### 2.5. Immunopathological analysis

Hematoxylin and eosin (HE) staining and immunostaining using antihuman alpha-smooth muscle actin ( $\alpha$ -SMA) (1A4; DAKO, Glostrup, Denmark), VEGF-A (sc-152, rabbit polyclonal, Santa Cruz, Heidelberg, Germany), CD3 (SP7; SPRING BIOSCIENCE, Pleasanton, CA, USA), CD20 (L26; DAKO), PD1 (programmed death 1, CD279) (ab52587, Abcam, Cambridge, MA, USA), CD138 (B-B4, Serotec, Raleigh, NC, USA), B cell lymphoma 6 (BCL6) (EP529Y; Epitomics, Burlingame, CA, USA), CD45RO (UCHL1, DAKO), immunoglobulin kappa (KP-53, Novocastra, Newcastle, UK) and lambda light chain (HP-6054, Novocastra) were performed. The presence of Epstein–Barr virus encoded RNA (EBER) was examined by in situ hybridization using EBER Probe (Leica Microsystems, Newcastle, UK) on formalin-fixed, paraffin-embedded sections. Double immunostaining analysis of human CD45RO and human BCL6 was performed as previously described [9]. Briefly, formalin-fixed, paraffin-embedded sections of AITL-affected spleen were immunostained using antibodies against human CD45RO and human BCL6. CD45RO protein in the membrane was

visualized in purple (Bajoran purple, Biocare Medical, Concord, CA, USA) and BCL6 protein in the nucleus was visualized in brown (DAB, Leica Microsystems).

### 2.6. Clonality assay

Clonal assessment of the AITL cells was performed using IdentiClone™ TCRB Gene Clonality Assay (*In vivo*Scribe Technologies, Inc., San Diego, CA, USA) according to the instructions of the manufacturer. Southern blotting analysis of T cell receptor C $\beta$ 1 gene was performed at SRL, Inc. (Tokyo, Japan).

### 2.7. Mouse serum protein

The mouse serum protein fraction was analyzed at SRL, Inc. Human immunoglobulin (Ig) G/A/M in mice serum were also measured at SRL, Inc.

## 3. Results

### 3.1. Establishment of the primary AITL cell-bearing NOG mouse model

Microscopic images of the affected lymph node of AITL patient 1 are shown in Fig. 1A. There was marked proliferation of arborizing

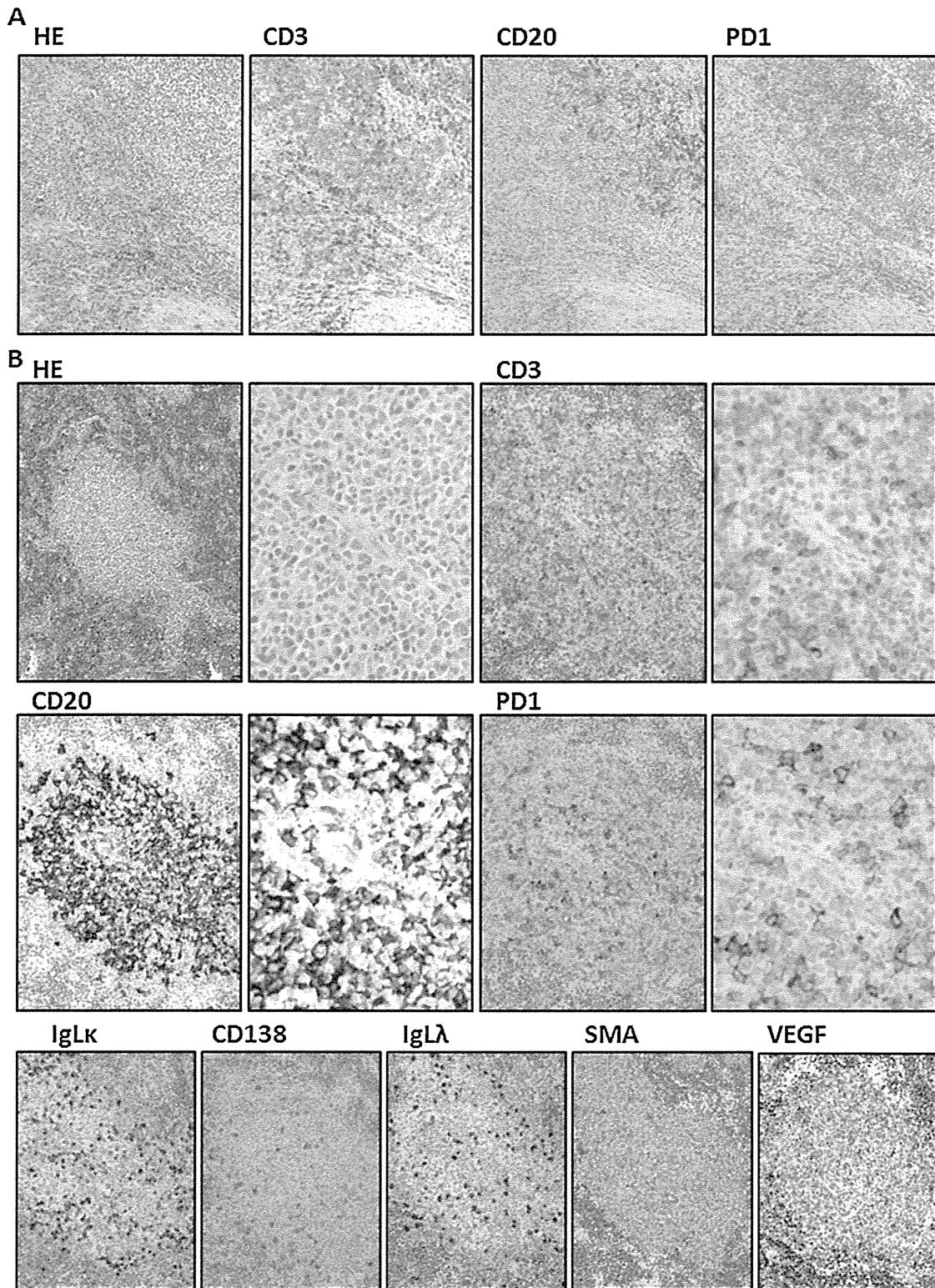


**Fig. 2.** Immunohistochemical analysis of primary AITL cell-bearing NOG mouse model. (A) Microscopic images with hematoxylin and eosin staining, and staining by anti-CD3, CD20, PD1, and CD138, of the affected lymph node of AITL patient 2 are shown. (B) Immunohistochemical images of sections of the spleen of a primary AITL-affected mouse that had been injected with affected lymph node cells from patient 2, with hematoxylin and eosin staining, and staining by anti-CD3, CD20, PD1, CD138, immunoglobulin kappa and lambda light chain, VEGF-A, and alpha-smooth muscle actin ( $\alpha$ -SMA).

high endothelial venules (HEV). There was polymorphic infiltrate composed of small to medium-sized lymphocytes with clear to pale cytoplasm, distinct cell membranes and minimal cytological atypia. The neoplastic cells were admixed with variable numbers of small reactive lymphocytes, eosinophils, plasma cells, and

histiocytes. These histological findings are typical of AITL [10]. NOG mice bearing AITL cells from patient 1 presented marked splenomegaly and mild hepatomegaly. The macroscopic appearance of a primary AITL cell-bearing NOG mouse from patient 1 is shown in Fig. 1B. Microscopic analysis revealed that the mice spleen

architectures were partially replaced by the infiltration of small to medium-sized lymphocytes with clear to pale cytoplasm, distinct cell membranes and minimal cytological atypia. The infiltrate also included plasma cells. Marked proliferation of HEV was seen in the spleen (Fig. 1C).

Flow cytometric analysis demonstrated that human CD3-positive T cells as well as CD19-positive B cells infiltrated into the spleen of the mice (Fig. 1D, left 2 panels). Both human T and B cells also infiltrated the mice bone marrow, but only T cells were detected in the blood (Fig. 1D, right 2 panels).

Microscopic images of the affected lymph node of AITL patient 2 are shown in Fig. 2A. There was polymorphic infiltrate composed of small to medium-sized lymphocytes including CD3-positive T cells as well as CD20-positive B cells. Some of the infiltrated cells were positive for PD1, which is known to be expressed on follicular helper T (TFH) cells [11,12] as well as AITL tumor cells [13]. These histological findings are also typical of AITL [10].

NOG mice bearing AITL cells from patient 2 presented marked splenomegaly and mild hepatomegaly. Immunohistochemical analyses of the AITL mice from patient 2 also demonstrated that the mice spleen architectures were partially replaced by the infiltration of small to medium-sized lymphocytes with clear to pale cytoplasm (Fig. 2B, upper left 2 panels). CD3-positive T cells (Fig. 2B, upper right 2 panels) as well as CD20-positive B cells (Fig. 2B, middle left 2 panels) infiltrated the mice spleen. Some of the infiltrated cells were positive for PD1 (Fig. 2B, middle right 2 panels). The infiltrated cells included CD138-positive plasma cells with no slanted distributions of immunoglobulin kappa or lambda light chain (Fig. 2B, lower left 3 panels). EBER-positive cells were not observed in the infiltrate (data not shown). There were abundant SMA-positive blood vessels in the spleen, and the infiltrate included VEGF-producing cells, most of which were AITL tumor cells (Fig. 2B, lower right 2 panels). These observations collectively indicated that the infiltrate consisted of PD1-positive AITL cells, a large number of reactive lymphocytes including both B and T cells, and polyclonal plasma cells, and there was marked vascular proliferation in the spleen. These immunohistological findings in the NOG AITL mice (Figs. 1C and 2B) were nearly identical to those in the respective donor AITL patients (Figs. 1A and 2A).

### 3.2. Human antibody production in the AITL NOG mice

Given the observation that there were abundant reactive human lymphocytes including B cells and plasma cells in AITL-affected mice spleen, we investigated whether they produced human Ig in the AITL NOG mice. As shown in Fig. 3A, significant Ig fractions and substantial amounts of human IgG/A/M were detected in the AITL mice from both donors. Double immunostaining revealed that human CD45RO- and BCL6-double-positive cells were detected in AITL-affected spleen (Fig. 3B). On the other hand, CD45RO<sup>-</sup>BCL6<sup>+</sup> cells were considered to be reactive B cells, because BCL6 is a transcriptional repressor expressed by germinal center B cells [14,15]. These observations collectively indicated that CD45RO<sup>+</sup>BCL6<sup>+</sup> AITL tumor cells helped antibody production by B cells or plasma cells. CD45RO<sup>+</sup>BCL6<sup>-</sup> cells were also detected in the spleen, and they were reactive T cells with memory phenotype [16].

### 3.3. Serial transplantations in AITL NOG mice

Suspensions of spleen cells from the mice receiving primary lymph node cells from AITL patient 1 were serially i.p. transplanted into fresh NOG mice. The second NOG mice were sacrificed when they became weakened. The second NOG mice presented marked splenomegaly and mild hepatomegaly (data not shown). Flow cytometric analysis demonstrated that human CD3-positive T cells, including both CD4 and CD8 cells, infiltrated into the mice liver,

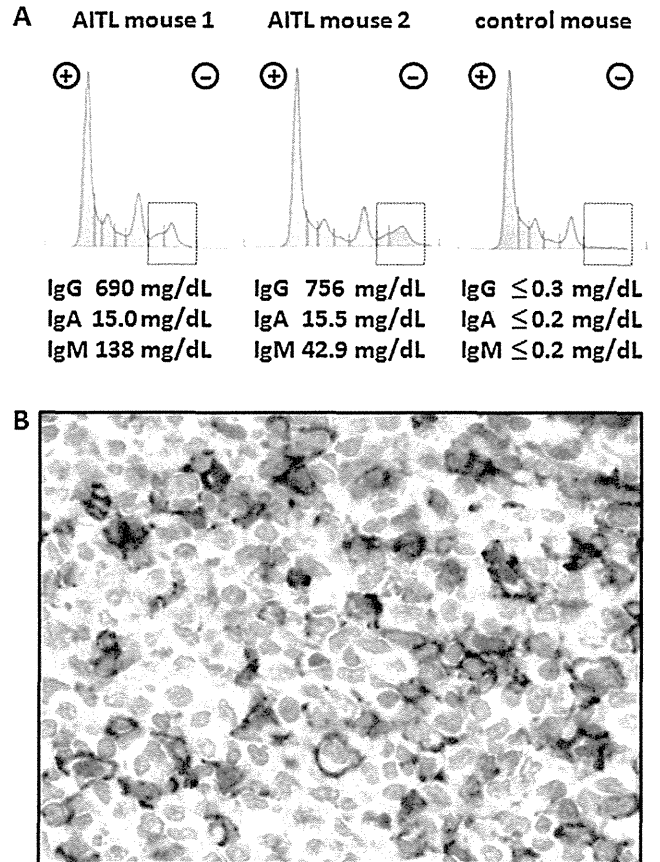


**Fig. 3.** Human antibody production in the AITL NOG mice. (A) Serum protein fractionation of NOG mice that had been injected with affected lymph node cells from AITL patient 1 and 2, and that of a naïve NOG mouse. (B) Double immunostaining analysis for human CD45RO and BCL6 in the AITL-affected mouse spleen. CD45RO in the membrane is visualized in purple and BCL6 in the nucleus is visualized in brown.

spleen, and bone marrow. In contrast to the first AITL mice, infiltration of B cells (CD4 and CD8 double negative cells) was not observed (Fig. 4A, left 6 panels). In the subsequent 3rd AITL mice, infiltration of CD8 cells was markedly decreased, and in the 4th AITL mice, the infiltrate of the liver, spleen, and bone marrow consisted of almost exclusively CD4-positive T cells (Fig. 4A, right 6 panels). Along with the disappearance of infiltrating B cells, human Ig was not detected in the sera of 2nd, 3rd and 4th AITL NOG mice (Fig. 4B). Clonality analysis by PCR detected clonal rearrangement of the T cell receptor in the affected lymph node from AITL patient 1 (Fig. 4C, top panel), which was confirmed by Southern blotting analysis of the T cell receptor C $\beta$ 1 gene (Fig. 4D, left panels, arrows). Clonality analysis by PCR demonstrated that there were two T cell clones in the spleen cells of the first AITL NOG mice, and the product size of one of these two was the same as that of the original AITL patient (Fig. 4C, upper 2 panels, arrows), indicating that a neoplastic T cell clone from the original AITL patient engrafted and proliferated in the first AITL NOG mice. This observation was confirmed by Southern blotting analysis (Fig. 4D, arrows). The same two T cell clones were detected in the 3rd and 4th AITL mice as those in the 1st AITL mice (Fig. 4C, lower 3 panels, arrows and arrowheads).

### 3.4. Macroscopic and microscopic findings of 4th AITL mice

The 4th AITL mice presented marked splenomegaly and mild hepatomegaly (Fig. 5A). Mice spleen architectures were almost wholly replaced by the infiltration of small to medium-sized lymphocytes with clear to pale cytoplasm. There was also marked



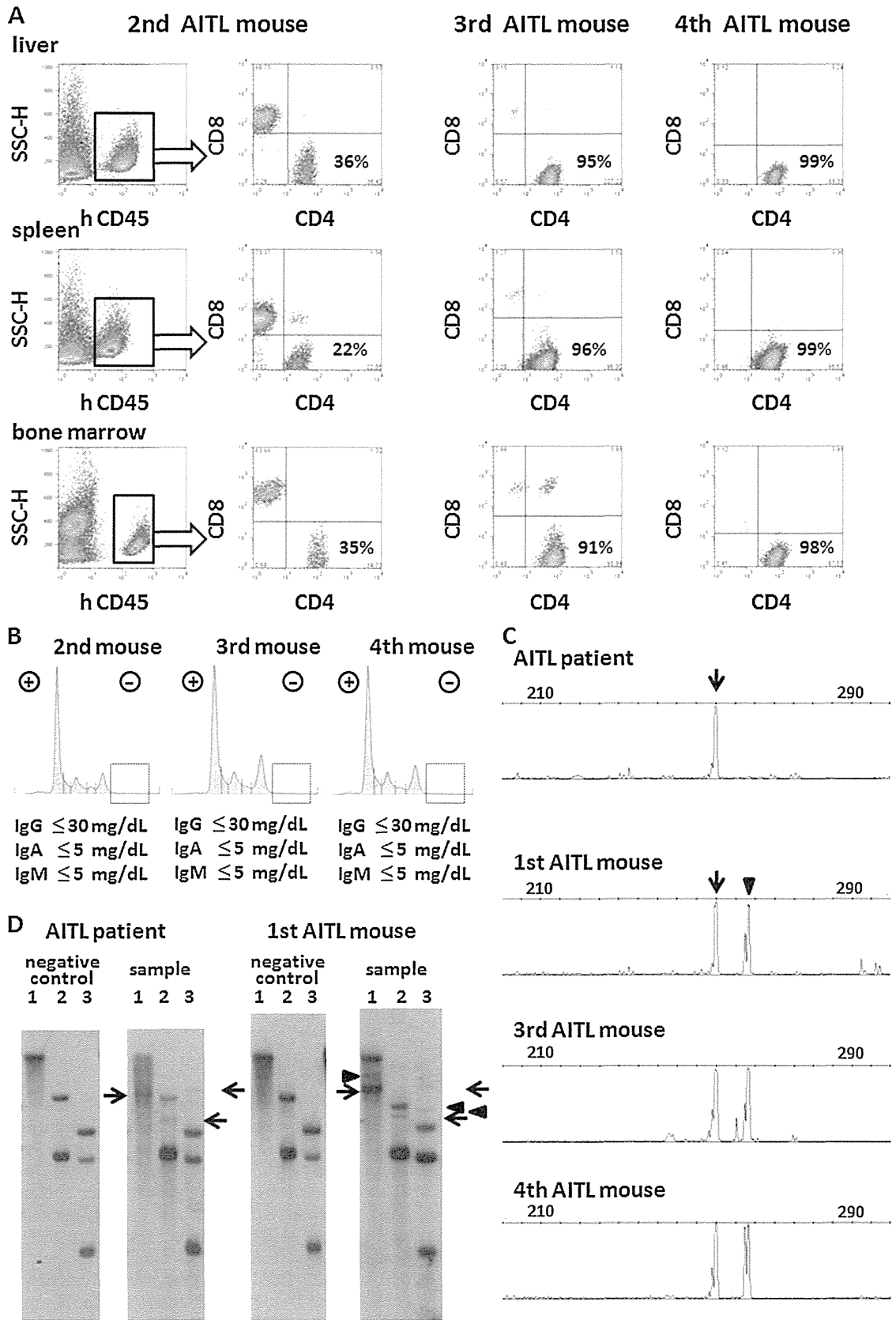


**Fig. 4.** Serial transplantations of spleen cells from AITL NOG mice. (A) The presence of human CD45-positive cells in the liver, spleen and bone marrow of the 2nd, 3rd, and 4th AITL NOG mice was determined by human CD4 and CD8 expression. (B) Serum protein fraction of 2nd, 3rd, and 4th AITL NOG mice. (C) Clonality analysis by PCR. Arrow and arrowhead indicate the clonal rearrangement of T cell receptor. (D) Clonality analysis by Southern blotting of T cell receptor C $\beta$ 1 gene. 1, 2, and 3 indicate BamH I, EcoR V, and Hind III, respectively. Arrow and arrowhead indicate the rearrangement band.

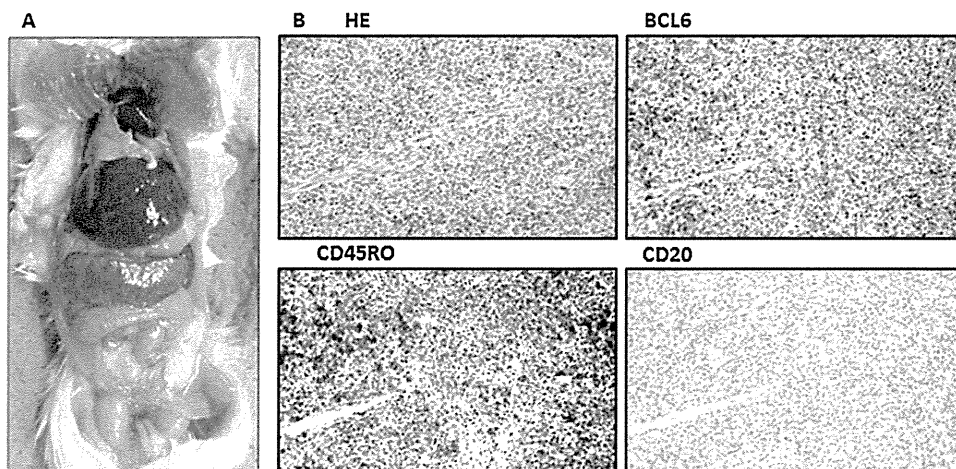


**Fig. 5.** Macroscopic and microscopic findings of 4th AITL mice. (A) Macroscopic image of a 4th AITL mouse. (B) Immunohistochemical images of the 4th AITL mouse spleen with hematoxylin and eosin staining, and staining by anti-BCL6, CD45RO, and CD20 antibodies.

vascular proliferation in the spleen. Most of the infiltrated cells were positive for CD45RO and BCL6. In contrast to the 1st AITL NOG mice, there were no CD20- (Fig. 5B) or CD138-positive reactive cells (data not shown), which were consistent with the results of flow cytometric analyses (Fig. 4A).

#### 4. Discussion

The recent identification of CD4<sup>+</sup> TFH cell as the cell of origin of AITL provides a rationale to explain some of the clinical and histological features of AITL. A fundamental function of TFH cells is regulation of B cell-mediated humoral immunity. It has been known that in humanized NOG mice reconstituted with human CD34<sup>+</sup> hematopoietic stem cells, there was little IgG production because of the inappropriate differentiation of human B cells in the mouse environment [17–20]. Considering this fact, it was striking that the present AITL NOG mice produced polyclonal human Ig including IgG. This was direct evidence that CD45RO<sup>+</sup>BCL6<sup>+</sup> AITL tumor cells functioned as TFH cells, and to the best of our knowledge, this is the first report to reconstitute TFH function in AITL cells in an experimental model either *in vitro* or *in vivo*. This could also explain one of the characteristic clinical features of AITL patients, hypergammaglobulinemia. In the AITL mice, human B cells were observed in the spleen and bone marrow, but not in blood, suggesting that antibody production mediated by T cells might need a suitable microenvironment like the germinal center of lymph nodes.

Serial transplantations of spleen cells of AITL NOG mice resulted in the reduction of reactive components such as B cell lineage and CD8-positive cells. CD4-positive AITL neoplastic cells can survive for a long period of time only by interacting with mouse environment cells. As a result, they failed to interact with human B or plasma cells, leading to the absence of human Ig production in the 2nd, 3rd, and 4th AITL NOG mice.

In general, not only monoclonal T cell receptor rearrangement, but also oligoclonal rearrangements were detected in AITL cases [1]. In the present study, although only one T cell clone (clone #1) was detected in an AITL patient 1, another T cell clone (clone #2) was also detected in the AITL NOG mice. We surmise that there were two neoplastic clones in the patient's affected lymph node, although the level of clone #2 was below the detectable limit. Because NOG mice have severe multiple immune dysfunctions, clone #2 was able to increase in the mice to a detectable level.

The immunohistological findings of the present AITL mice were almost identical to those of AITL patients; i.e., only a fraction of

AITL neoplastic cells, which were small to medium-sized cells with clear cytoplasm and minimal cytologic atypia, were admixed with a reactive population of small lymphocytes including B and T cells, and plasma cells, and the spleen showed prominent vascularization. On the other hand, there was a lack of myeloid lineage cells such as eosinophils, histiocytes, and follicular dendritic cells, in the background inflammatory components, probably due to their fundamentally short life span. There was also a lack of EBV-positive B cells in the infiltrate in the present AITL mice, which could be explained by the fact that there was a lack of EBV-positive B cells in the background inflammatory components in the affected lymph node of both donors. In this type of analysis, attention should be paid to cross-reaction of antihuman antigens antibodies to mouse cells. The antihuman CD3, CD20, PD1, CD138, BCL6, CD45RO, immunoglobulin kappa and lambda light chain antibodies in the present study did not react with hematopoietic cells of mice origin (data not shown), probably due to the lack of mice T, B, and NK cells in NOG mice [7,8].

In conclusion, primary AITL tumor cells and reactive components engrafted NOG mice, and AITL cells interacted with B and plasma cells, and functioned as TFH cells. Human Igs including IgG were produced in the mice. The present observations strongly support the recent identification of TFH cell as the cell of origin of AITL. The present procedures using NOG mice would be a powerful tool to understand the immunopathogenesis of AITL.

#### Grants support

The present study was supported by Grants-in-Aid for Young Scientists (A) (No. 22689029, T. Ishida), Scientific Research (B) (No. 22300333, T. Ishida, and R. Ueda), and Scientific Support Programs for Cancer Research (No. 221S0001, T. Ishida) from the Ministry of Education, Culture, Sports, Science and Technology of Japan, Grants-in-Aid for National Cancer Center Research and Development Fund (No. 21-6-3, T. Ishida), and Health and Labour Sciences Research Grants (H22-Clinical Cancer Research-general-028, T. Ishida, and H23-Third Term Comprehensive Control Research for Cancer-general-011, T. Ishida, and H. Inagaki) from the Ministry of Health, Labour and Welfare, Japan.

#### Conflicts of interest

Nagoya City University Graduate School of Medical Sciences has received research grant support from Kyowa Hakko Kirin for works

provided by Takashi Ishida. No other conflict of interest relevant to this article is reported.

### Acknowledgements

We thank Ms. Chiori Fukuyama for her excellent technical assistance, and Ms. Naomi Ochiai for her excellent secretarial assistance.

*Authors' contributions.* F.S., T.I., R.U., and H.I. designed the research. F.S., T.I., A.I., F.M., A.M., and H.T. performed the experiments. All of the authors analyzed and interpreted the data. F.S. and T.I. wrote the paper, and all of the other authors contributed to writing the paper.

### References

- [1] de Leval L, Gisselbrecht C, Gaulard P. Advances in the understanding and management of angioimmunoblastic T-cell lymphoma. *Br J Haematol* 2010;148:673–89.
- [2] Barabe F, Kennedy JA, Hope KJ, Dick JE. Modeling the initiation and progression of human acute leukemia in mice. *Science* 2007;316:600–4.
- [3] Ishikawa F, Yoshida S, Saito Y, Hijikata A, Kitamura H, Tanaka S, et al. Chemotherapy resistant human AML stem cells home to and engraft within the bone-marrow endosteal region. *Nat Biotechnol* 2007;25:1315–21.
- [4] Mori F, Ishida T, Ito A, Sato F, Masaki A, Takino H, et al. Potent antitumor effects of bevacizumab in a microenvironment-dependent human lymphoma mouse model. *Blood Cancer J* 2012;2:e67.
- [5] Sato K, Misawa N, Nie C, Satou Y, Iwakiri D, Matsuoka M, et al. A novel animal model of Epstein–Barr virus-associated hemophagocytic lymphohistiocytosis in humanized mice. *Blood* 2011;117:5663–73.
- [6] Ito A, Ishida T, Utsunomiya A, Sato F, Mori F, Yano H, et al. Defucosylated anti-CCR4 monoclonal antibody exerts potent ADCC against primary ATLL cells mediated by autologous human immune cells in NOD/Shi-scid, IL-2R gamma(null) mice in vivo. *J Immunol* 2009;183:4782–91.
- [7] Ito M, Hiramatsu H, Kobayashi K, Suzue K, Kawahata M, Hioki K, et al. NOD/SCID/gamma null mouse: an excellent recipient mouse model for engraftment of human cells. *Blood* 2002;100:3175–82.
- [8] Ito M, Kobayashi K, Nakahata T. NOD/Shi-scid IL2rynull (NOG) mice more appropriate for humanized mouse models. *Curr Top Microbiol Immunol* 2008;324:53–76.
- [9] Ishida T, Ishii T, Inagaki A, Yano H, Komatsu H, Iida S, et al. Specific recruitment of CC chemokine receptor 4-positive regulatory T cells in Hodgkin lymphoma fosters immune privilege. *Cancer Res* 2006;66:5716–22.
- [10] Dogan A, Gaulard P, Jaffe ES, Ralfkiaer E, Muller-Hermelink HK. Angioimmunoblastic T-cell lymphoma. In: Swerdlow SH, Campo E, Harris NL, Jaffe ES, Pileri SA, Stein H, Thiele J, Vardiman JW, editors. WHO classification of tumours of haematopoietic and lymphoid tissues. Lyon: IARC; 2008. p. 309.
- [11] Fazilleau N, McHeyzer-Williams LJ, Rosen H, McHeyzer-Williams MG. The function of follicular helper T cells is regulated by the strength of T cell antigen receptor binding. *Nat Immunol* 2009;10:375–84.
- [12] Haynes NM, Allen CD, Lesley R, Ansel KM, Killeen N, Cyster JG. Role of CXCR5 and CCR7 in follicular Th cell positioning and appearance of a programmed cell death gene-1high germinal center-associated subpopulation. *J Immunol* 2007;179:5099–108.
- [13] Roncador G, García Verdes-Montenegro JF, Tedoldi S, Paterson JC, Klapper W, Ballabio E, et al. Expression of two markers of germinal center T cells (SAP and PD-1) in angioimmunoblastic T-cell lymphoma. *Haematologica* 2007;92:1059–66.
- [14] Crotty S, Johnston RJ, Schoenberger SP. Effectors and memories: Bcl-6 and Blimp-1 in T and B lymphocyte differentiation. *Nat Immunol* 2010;11:114–20.
- [15] Klein U, Dalla-Favera R. Germinal centres: role in B-cell physiology and malignancy. *Nat Rev Immunol* 2008;8:22–33.
- [16] Akbar AN, Terry L, Timms A, Beverley PC, Janossy G. Loss of CD45R and gain of UCHL1 reactivity is a feature of primed T cells. *J Immunol* 1988;140:2171–8.
- [17] Ishikawa F, Yasukawa M, Lyons B, Yoshida S, Miyamoto T, Yoshimoto G, et al. Development of functional human blood and immune systems in NOD/SCID/IL2 receptor {gamma} chain(null) mice. *Blood* 2005;106:1565–73.
- [18] Matsumura T, Kametani Y, Ando K, Hirano Y, Katano I, Ito R, et al. Functional CD5+ B cells develop predominantly in the spleen of NOD/SCID/gammac(null) (NOG) mice transplanted either with human umbilical cord blood, bone marrow, or mobilized peripheral blood CD34+ cells. *Exp Hematol* 2003;31:789–97.
- [19] Traggiai E, Chicha L, Mazzucchelli L, Bronz L, Piffaretti JC, Lanzavecchia A, et al. Development of a human adaptive immune system in cord blood cell-transplanted mice. *Science* 2004;304:104–7.
- [20] Watanabe Y, Takahashi T, Okajima A, Shiokawa M, Ishii N, Katano I, et al. The analysis of the functions of human B and T cells in humanized NOD/shi-scid/gammac(null) (NOG) mice (hu-HSC NOG mice). *Int Immunol* 2009;21:843–58.



## Case Report

## Stevens–Johnson Syndrome associated with mogamulizumab treatment of adult T-cell leukemia/lymphoma

Takashi Ishida,<sup>1,6</sup> Asahi Ito,<sup>1</sup> Fumihiko Sato,<sup>2</sup> Shigeru Kusumoto,<sup>1</sup> Shinsuke Iida,<sup>1</sup> Hiroshi Inagaki,<sup>2</sup> Akimichi Morita,<sup>3</sup> Shiro Akinaga<sup>4</sup> and Ryuzo Ueda<sup>5</sup>Departments of <sup>1</sup>Medical Oncology and Immunology, <sup>2</sup>Anatomic Pathology and Molecular Diagnostics, <sup>3</sup>Geriatric and Environmental Dermatology, Nagoya City University Graduate School of Medical Sciences, Nagoya; <sup>4</sup>Kyowa Hakko Kirin, Tokyo; <sup>5</sup>Department of Tumor Immunology, Aichi Medical University School of Medicine, Nagakute, Japan

(Received December 25, 2012/Revised January 21, 2013/Accepted January 23, 2013/Accepted manuscript online January 30, 2013)

We report an adult T-cell leukemia/lymphoma patient suffering from Stevens–Johnson Syndrome (SJS) during mogamulizumab (humanized anti-CCR4 monoclonal antibody) treatment. There was a durable significant reduction of the CD4<sup>+</sup>CD25<sup>high</sup>FOXP3<sup>+</sup> regulatory T (Treg) cell subset in the patient's PBMC, and the affected inflamed skin almost completely lacked FOXP3-positive cells. This implies an association between reduction of the Treg subset by mogamulizumab and occurrence of SJS. The present case should contribute not only to our understanding of human pathology resulting from therapeutic depletion of Treg cells, but also alert us to the possibility of immune-related severe adverse events such as SJS when using mogamulizumab. We are currently conducting a clinical trial of mogamulizumab for CCR4-negative solid cancers (UMIN000010050), specifically aiming to deplete Treg cells. (*Cancer Sci* 2013; 104: 647–650)

Adult T-cell leukemia/lymphoma (ATL) is an aggressive peripheral T-cell neoplasm caused by HTLV-1. The disease is resistant to conventional chemotherapeutic agents, and has a very poor prognosis.<sup>(1)</sup> Mogamulizumab (KW-0761) is a defucosylated humanized monoclonal antibody targeting CC chemokine receptor 4 (CCR4).<sup>(2)</sup> A phase I clinical trial for relapsed CCR4-positive peripheral T-cell neoplasms, including ATL, and a phase II study for relapsed ATL have been conducted with mogamulizumab.<sup>(3,4)</sup> This agent was subsequently approved for the treatment of relapsed or refractory ATL in Japan, the first country in the world to do so, in March 2012. Mogamulizumab went on sale on 29 May 2012. The interim report for the post-marketing surveillance from 29 May to 28 September 2012 revealed skin-related severe adverse events (SAE), as defined by the Medical Dictionary for Regulatory Activities Terminology/Japan, in nine patients. Thus, during only the first 4 months of use, 9 skin-related SAE, including 4 cases of Stevens–Johnson Syndrome (SJS)/toxic epidermal necrolysis (TEN) were reported, with 1 SJS/TEN fatality. These skin-related, potentially fatal SAE are certainly a challenge to the free use of this agent and clearly require investigation. Therefore, here we report an informative ATL patient suffering from SJS on mogamulizumab treatment, focusing on the reduction of the regulatory T (Treg) cell subset (CD4<sup>+</sup>CD25<sup>high</sup>FOXP3<sup>+</sup>) caused by the antibody.

## Case Report

A 71-year old woman was admitted due to elevation of her lymphocyte count. She had been diagnosed as suffering from

acute-type ATL nearly 5 months prior to admission. She had received VCAP-AMP-VECP chemotherapy<sup>(5)</sup> followed by oral sobuzoxane in another hospital, and achieved a transient partial remission. We started mogamulizumab to treat the flare-up of ATL disease (Fig. 1). Grade 1 skin eruptions appeared around her neck after three antibody infusions. Because we were also giving her antibacterial (ciprofloxacin hydrochloride), fungal (itraconazole), pneumocystic (sulfamethoxazole-trimethoprim) and viral (aciclovir) prophylaxes in addition to stomach medicine (lansoprazole), we judged the skin event to be due to drug eruption caused by one of these concomitant drugs. Therefore, we stopped all five, but continued with mogamulizumab. Despite their discontinuation and treatment with topical steroids, the skin rashes continued to worsen. We started the patient on 30 mg oral prednisolone, which improved the skin symptoms. The patient was then able to complete the eight planned infusions, and oral prednisolone was tapered off. She was discharged from hospital 8 days after her eighth infusion (day 65), and thereafter seen as an outpatient. However, she had to be readmitted as an emergency patient at day 75 because of fulminant skin rashes. These included erythemas, scale-like plaques, vesicles, blisters and erosions over many areas of the body. Her lips were swollen and oral mucosa was erosive (Fig. 2a). Skin biopsy revealed marked liquefaction, degeneration and perivascular inflammation with dominant CD8-positive cells but almost complete lack of FOXP3-positive cells (Fig. 2b). We diagnosed her as a SJS, and immediately started steroid pulse therapy (methylprednisolone 500 mg/day ×3 days), followed by oral prednisolone. Her skin and mucosal lesions improved gradually, and became inactive. At the same time, her general condition improved. Thus, we again tapered the steroid dose, and she was discharged at day 144. However, she had to come back yet again as an emergency patient on day 151 for the same reason as before, with fulminant skin rashes. We prescribed her mini-steroid pulse therapy (methylprednisolone 125 mg/day ×1 day), followed by oral prednisolone. Once more, her skin lesions improved gradually. Over this whole period, complete ATL remission was maintained by mogamulizumab. The HTLV-1 provirus load in PBMC pre-treatment, and at days 121 and 162 was 750.1, 0.0 (under the limit of detection) and 0.8 copies/1000 cells, respectively. These post-treatment values are strikingly low, considering that median HTLV-1

<sup>6</sup>To whom correspondence should be addressed.  
E-mail: itakashi@med.nagoya-cu.ac.jp

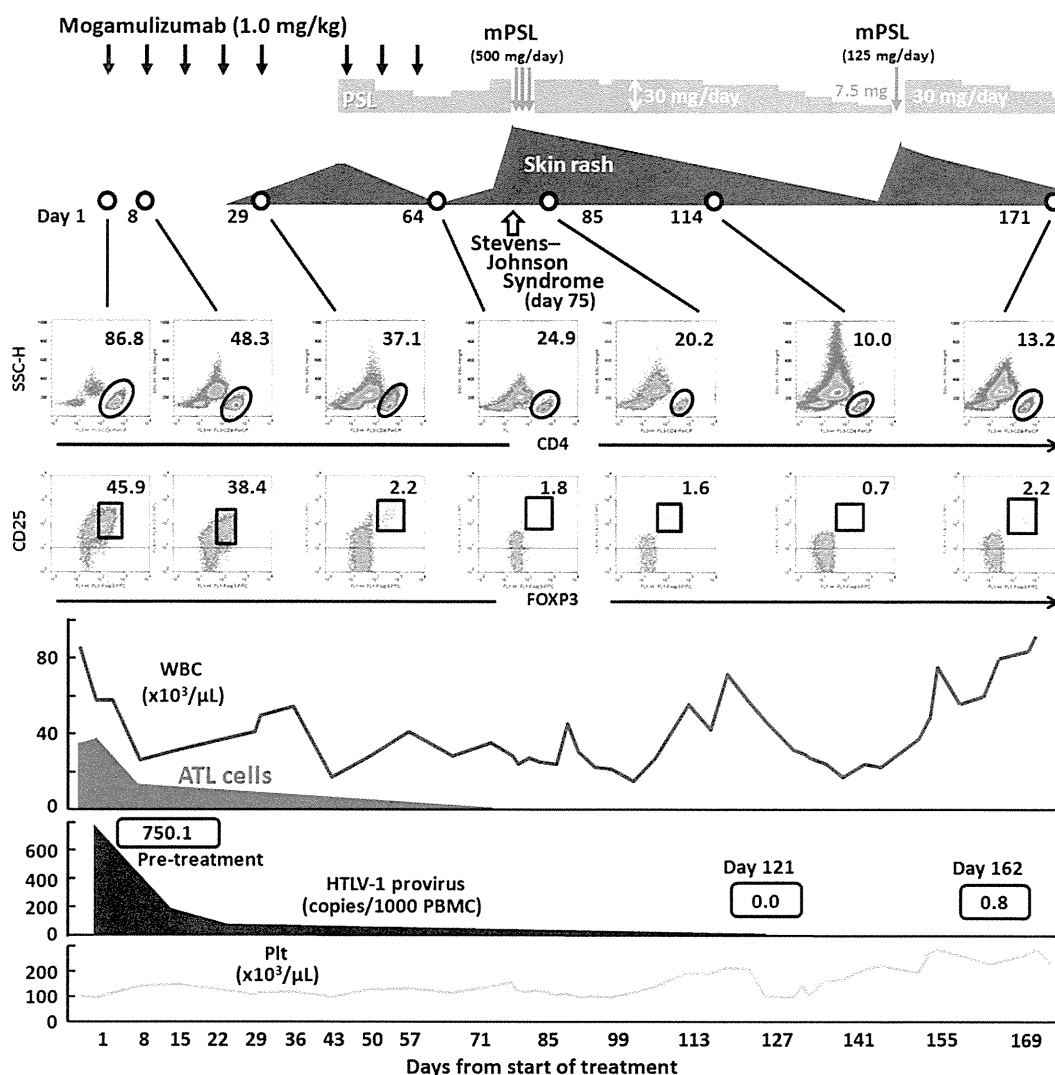


Fig. 1. Clinical course of an ATL patient receiving mogamulizumab monotherapy. ATL; adult T-cell leukemia/lymphoma; mPSL, methylprednisolone; Plt, platelet PSL; prednisolone; WBC, white blood cell.

load in asymptomatic carriers reported by other investigators is 18.0 copies/1000 cells.<sup>(6)</sup>

We also analyzed CD4, CD25 and FOXP3 expression by PBMC during and after antibody treatment (Fig. 1, middle panels). Before treatment, the majority of the patient's PBMC consisted of CD4-positive and CD25-positive ATL cells. Just before the 5th antibody infusion (day 29), around the time when her skin rash first appeared, the proportion of CD25<sup>high</sup>-FOXP3<sup>+</sup>/CD4<sup>+</sup> cells was markedly reduced, to 2.2%. This is low even compared to healthy individuals (CD25<sup>high</sup>-FOXP3<sup>+</sup>/CD4<sup>+</sup> cells, mean 3.3%, median 3.3%, range 2.6–4.4%) (Fig. 3). Around the time of SJS onset, the proportion of cells in the Treg subset was further reduced. The proportion of CD25<sup>high</sup>FOXP3<sup>+</sup>/CD4<sup>+</sup> cells at days 64, 85 and 114 was 1.8%, 1.6% and 0.7%, respectively. The striking reduction of the Treg subset persisted until 4 months after the last of the eight antibody infusions (day 171).

## Discussion

Drugs often induce adverse cutaneous reactions of varying severity, ranging from simple uncomplicated eruptions to potentially fatal eruptions, such as SJS and TEN, within the

spectrum of severe adverse reactions affecting skin and mucosa. Although many factors that might cause variability in the clinical course of such adverse reactions have been suggested, it remains unknown which factors are predominantly involved in these processes. The most prevalent severe drug eruptions are thought to be mediated by drug-reactive T-cells,<sup>(7)</sup> although we also need to be aware of the alternative view that severe drug eruptions are due to a dysregulated immune system. In this regard, an effect mediated by Treg cells is a likely candidate in severe drug eruptions. Indeed, it is reported that Treg cells can prevent experimentally-induced epidermal injury mimicking TEN in an animal model.<sup>(8)</sup> Furthermore, Takahashi *et al.* (2009) report that Treg cell function is profoundly impaired in patients with TEN.<sup>(9)</sup> Consistent with these reports, a marked reduction of the Treg subset was observed in the present case.

Mogamulizumab is the first therapeutic agent targeting CCR4, which is expressed on Treg cells,<sup>(10,11)</sup> to receive marketing approval anywhere in the world. The reduction of the Treg subset seen here was not specific to the present case, but is commonly observed in ATL patients receiving mogamulizumab. In fact, skin rashes were observed as a frequent non-hematologic adverse event (AE) (63%), mostly occurring

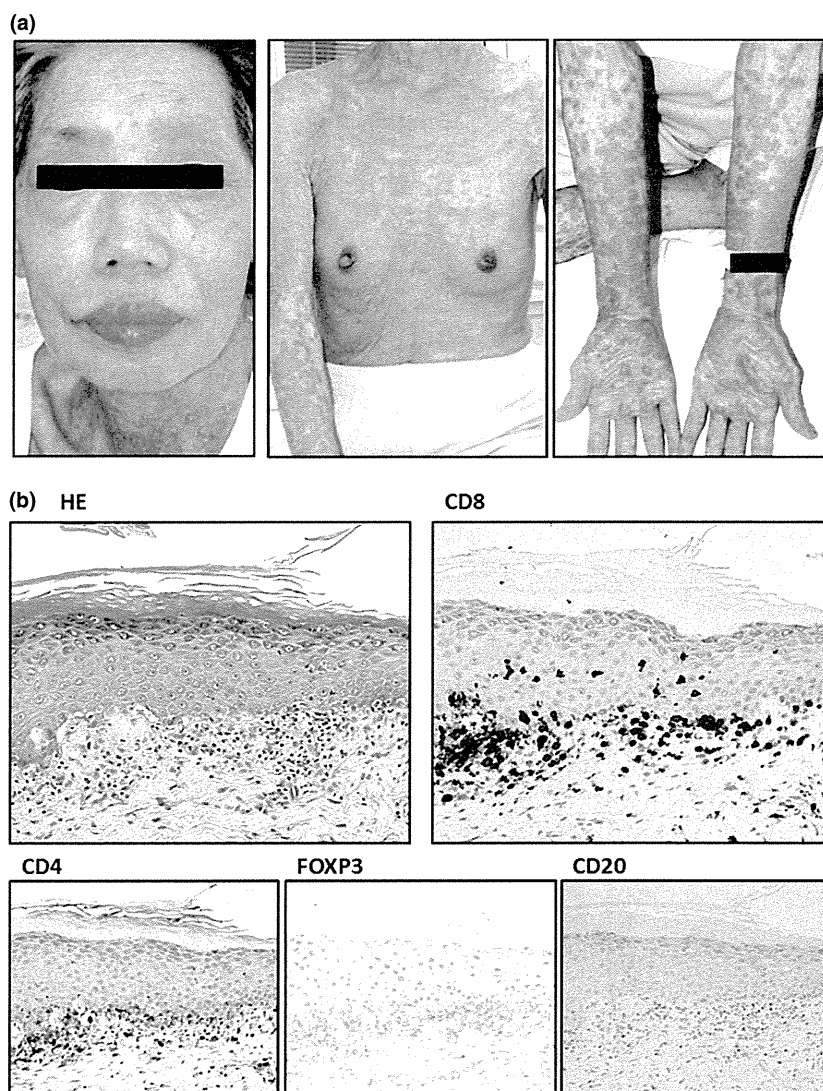


**Fig. 2.** (a) Macroscopic observations of the patient's skin on the day she was diagnosed with Stevens–Johnson Syndrome. (b) Corresponding skin biopsy showing liquefaction, degeneration and perivascular inflammation with dominant CD8-positive cells but almost no FOXP3-positive cells.

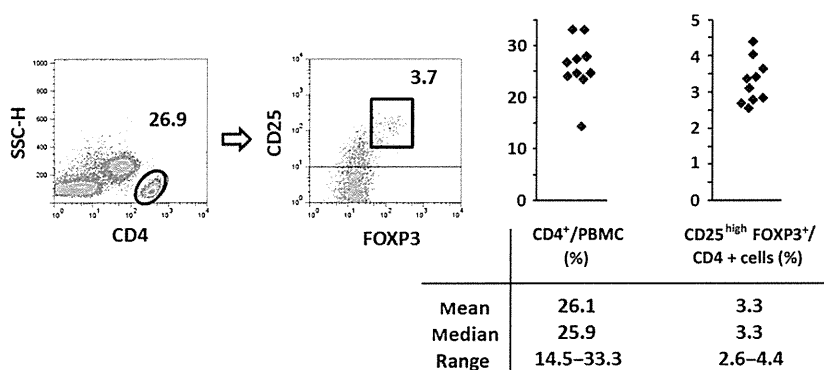


**Fig. 3.** CD4<sup>+</sup>CD25<sup>high</sup>FOXP3<sup>+</sup> regulatory T cells in PBMC from healthy volunteers ( $n = 10$ ).

after the fourth or subsequent infusions in the phase II study.<sup>(4)</sup> The present case was one of these patients. It has been reported that alterations in CD4<sup>+</sup>CD25<sup>+</sup>FOXP3<sup>+</sup> Treg cell frequencies and/or function may contribute to various types of autoimmune diseases.<sup>(12)</sup> Because the CCR4 molecule aids lymphocyte skin-specific homing,<sup>(13)</sup> it is not unexpected

that skin rashes, which could be an immune-related AE, will be frequently observed in ATL patients receiving mogamulizumab. Because it is an urgent issue to identify which factors determine the severity of immune-related skin disorders associated with mogamulizumab treatment, further investigation on this matter are clearly warranted.

However, reduction of Treg cells is a promising strategy for boosting antitumor immunity in cancer patients, because these cells are increased in the tumor microenvironment and may play an important role in tumor escape from host immunity in several different types of cancer.<sup>(14,15)</sup> Thus, reduction of Treg cells by mogamulizumab in cancer patients would have both potential benefits leading to enhanced antitumor immunity, but also pose risks of autoimmune disease. The skin-related SAE, including SJS/TEN, are representative of the latter. Currently, several clinical trials of mogamulizumab are being conducted worldwide, not only for ATL, but also other types of lymphoma. In addition, we are currently conducting a clinical trial of mogamulizumab for CCR4-negative solid cancers (UMIN000010050), specifically aiming to deplete Treg cells. Therefore, it is a matter of some urgency to establish the safest and most effective treatment strategies for using mogamulizumab not only in ATL patients but also other types of cancer, to maximize benefit and minimize risk.

In summary, the present case should contribute not only to our understanding of human pathology resulting from therapeutic depletion of Treg cells, but also alert us to the possibility of immune-related SAE, such as SJS/TEN, when using mogamulizumab.

## References

- Ishida T, Ueda R. Antibody therapy for Adult T-cell leukemia-lymphoma. *Int J Hematol* 2011; **94**: 443–52.
- Ishii T, Ishida T, Utsunomiya A *et al.* Defucosylated humanized anti-CCR4 monoclonal antibody KW-0761 as a novel immunotherapeutic agent for adult T-cell leukemia/lymphoma. *Clin Cancer Res* 2010; **16**: 1520–31.
- Yamamoto K, Utsunomiya A, Tobinai K *et al.* Phase I study of KW-0761, a defucosylated humanized anti-CCR4 antibody, in relapsed patients with adult T-cell leukemia-lymphoma and peripheral T-cell lymphoma. *J Clin Oncol* 2010; **28**: 1591–8.
- Ishida T, Joh T, Uike N *et al.* Defucosylated anti-CCR4 monoclonal antibody (KW-0761) for relapsed adult T-cell leukemia-lymphoma: a multicenter phase ii study. *J Clin Oncol* 2012; **30**: 837–42.
- Tsukasaki K, Utsunomiya A, Fukuda H *et al.* VCAP-AMP-VECP compared with biweekly CHOP for adult T-cell leukemia-lymphoma: Japan Clinical Oncology Group Study JCOG9801. *J Clin Oncol* 2007; **25**: 5458–64.
- Sonoda J, Koriyama C, Yamamoto S *et al.* HTLV-1 provirus load in peripheral blood lymphocytes of HTLV-1 carriers is diminished by green tea drinking. *Cancer Sci* 2004; **95**: 596–601.
- Nassif A, Bensussan A, Boumsell L *et al.* Toxic epidermal necrolysis: effector cells are drug-specific cytotoxic T cells. *J Allergy Clin Immunol* 2004; **114**: 1209–15.
- Azukizawa H, Sano S, Kosaka H, Sumikawa Y, Itami S. Prevention of toxic epidermal necrolysis by regulatory T cells. *Eur J Immunol* 2005; **35**: 1722–30.
- Takahashi R, Kano Y, Yamazaki Y, Kimishima M, Mizukawa Y, Shiohara T. Defective regulatory T cells in patients with severe drug eruptions: timing of the dysfunction is associated with the pathological phenotype and outcome. *J Immunol* 2009; **182**: 8071–9.
- Iellem A, Mariani M, Lang R *et al.* Unique chemotactic response profile and specific expression of chemokine receptors CCR4 and CCR8 by CD4(+) CD25(+) regulatory T cells. *J Exp Med* 2001; **194**: 847–53.
- Ishida T, Ishii T, Inagaki A *et al.* Specific recruitment of CC chemokine receptor 4-positive regulatory T cells in Hodgkin lymphoma fosters immune privilege. *Cancer Res* 2006; **66**: 5716–22.
- Michels-van Amelsfort JM, Walter GJ, Taams LS. CD4<sup>+</sup> CD25<sup>+</sup> regulatory T cells in systemic sclerosis and other rheumatic diseases. *Expert Rev Clin Immunol* 2011; **7**: 499–514.
- Campbell JJ, Haraldsen G, Pan J *et al.* The chemokine receptor CCR4 in vascular recognition by cutaneous but not intestinal memory T cells. *Nature* 1999; **400**: 776–80.
- Jacobs JF, Nierkens S, Figdor CG, de Vries IJ, Adema GJ. Regulatory T cells in melanoma: the final hurdle towards effective immunotherapy? *Lancet Oncol* 2012; **13**: e32–42.
- Ishida T, Ueda R. Immunopathogenesis of lymphoma: focus on CCR4. *Cancer Sci* 2011; **102**: 44–50.

## Acknowledgments

The authors thank the husband of the patient for consenting to the publication of her clinical details. The present study was supported by Grants-in-Aid for Young Scientists (A) (No. 22689029), Scientific Research (B) (No. 22300333), and Scientific Support Programs for Cancer Research (No. 221S0001) from the Ministry of Education, Culture, Sports, Science and Technology of Japan, a Grant-in-Aid from the National Cancer Center Research and Development Fund (No. 23-A-17), and Health and Labour Sciences Research Grants (H22-Clinical Cancer Research-general-028 and H23-Third Term Comprehensive Control Research for Cancer-general-011) from the Ministry of Health, Labour and Welfare, Japan.

## Disclosure Statement

Nagoya City University Graduate School of Medical Sciences has received research grant support from Kyowa Hakko Kirin for works provided by Takashi Ishida. Takashi Ishida received honoraria from Kyowa Hakko Kirin for his works. Shiro Akinaga is an employee of Kyowa Hakko Kirin. No other conflict of interest relevant to this article is reported.

**Case Report**

# Reactivation of hepatitis B virus in a patient with adult T-cell leukemia–lymphoma receiving the anti-CC chemokine receptor 4 antibody mogamulizumab

Nobuaki Nakano,<sup>1</sup> Shigeru Kusumoto,<sup>2</sup> Yasuhito Tanaka,<sup>3</sup> Takashi Ishida,<sup>2</sup> Shogo Takeuchi,<sup>1</sup> Yoshifusa Takatsuka,<sup>1</sup> Shiro Akinaga,<sup>4</sup> Masashi Mizokami,<sup>5</sup> Ryuzo Ueda<sup>6</sup> and Atea Utsunomiya<sup>1</sup>

<sup>1</sup>Department of Hematology, Imamura Bun-in Hospital, Kagoshima, Departments of <sup>2</sup>Medical Oncology and Immunology and <sup>3</sup>Virology and Liver Unit, Nagoya City University Graduate School of Medical Sciences, Nagoya, <sup>4</sup>Kyowa Hakko Kirin., Tokyo, <sup>5</sup>The Research Center for Hepatitis and Immunology, National Center for Global Health and Medicine, Ichikawa, and <sup>6</sup>Department of Tumor Immunology, Aichi Medical University School of Medicine, Aichi, Japan

The introduction of molecularly targeted drugs has increased the risk of reactivation of hepatitis B virus (HBV), which is a potentially fatal complication following anticancer chemotherapy even in patients who have previously resolved their HBV infection. CC chemokine receptor 4 (CCR4) has been identified as a novel molecular target in antibody therapy for patients with adult T-cell leukemia–lymphoma (ATL) and peripheral T-cell lymphoma, and the humanized anti-CCR4 monoclonal antibody mogamulizumab has been developed. We reported HBV reactivation of an ATL patient with

previously resolved HBV infection after mogamulizumab treatment in a dose-finding study for this antibody. Our retrospective analysis using preserved samples also revealed the detailed kinetics of HBV DNA levels before and just after HBV reactivation.

**Key words:** CC chemokine receptor 4, hepatitis B virus, mogamulizumab, reactivation

**INTRODUCTION**

REACTIVATION OF HEPATITIS B virus (HBV) following anticancer chemotherapy and immunosuppressive therapy is a potentially fatal complication that needs to be followed up carefully.<sup>1</sup> The advent of

molecularly targeted drugs, which have immunosuppressive or immunomodulating actions, has increased the risk of HBV reactivation. The anti-CD20 monoclonal antibody rituximab, which forms part of the standard regimen for B-cell non-Hodgkin's lymphoma, has the potential to cause HBV reactivation, even in patients who have previously resolved their HBV infection and are hepatitis B surface antigen (HBsAg) negative at baseline.<sup>2–6</sup> CC chemokine receptor 4 (CCR4) has been identified as a novel molecular target in antibody therapy for patients with adult T-cell leukemia–lymphoma (ATL) and peripheral T-cell lymphoma, and the humanized anti-CCR4 monoclonal antibody mogamulizumab, the Fc region of which is de-fucosylated to enhance antibody-dependent cellular cytotoxicity, has been developed.<sup>7–10</sup> We herein report HBV reactivation of an ATL patient with previously resolved HBV infection after mogamulizumab treatment in a dose-finding study for this antibody.

*Correspondence:* Dr Shigeru Kusumoto, Department of Medical Oncology and Immunology, Nagoya City University Graduate School of Medical Sciences, 1 Kawasumi, Mizuho-chou, Mizuho-ku, Nagoya, Aichi 467-8601, Japan. Email: skusumot@med.nagoya-cu.ac.jp

*Conflict of interest:* S. K., research funding from Kyowa Hakko Kirin and honoraria from Bristol-Myers Squibb; Y. T., research funding and honoraria from Bristol-Myers Squibb; T. I., research funding and honoraria from Kyowa Hakko Kirin; S. A., employment from Kyowa Hakko Kirin; R. U., research funding from Kyowa Hakko Kirin; and A. U., advisory role and honoraria from Kyowa Hakko Kirin.

Received 7 March 2013; revision 17 March 2013; accepted 20 March 2013.

**CASE REPORT**

**A** 65-YEAR-OLD JAPANESE woman complained of persistent fatigue and weight loss of 8 kg in 2 weeks. The laboratory findings showed that her white blood cell count was elevated to 16 800/ $\mu$ L, of which abnormal lymphocytes accounted for 18%, and seropositivity for human T-cell leukemia virus type-1 (HTLV-1). Monoclonal integration of HTLV-1 was revealed by Southern blotting of DNA from peripheral blood. She was diagnosed as ATL, chronic type, in April 2004. Since then, she had experienced repeating infectious episodes and systemic lymph node swelling. On April 2005, she

began to receive systemic chemotherapy composed of sobuzoxane (400 mg/day), etoposide (25 mg/day) and prednisolone (10 mg/day) p.o. twice a week because of disease progression to acute type which was accompanied by new ATL involvement in her right breast region and right axilla lymphadenopathy. As her disease was refractory to this regimen, she received four cycles of THP-COP regimen (cyclophosphamide, pirarubicin, vincristine and prednisolone) from August 2005 through October 2005 (Fig. 1a). She achieved a partial response and was followed up without subsequent chemotherapy including steroids for 1.4 years, but her disease progressed with markedly increased ATL cells

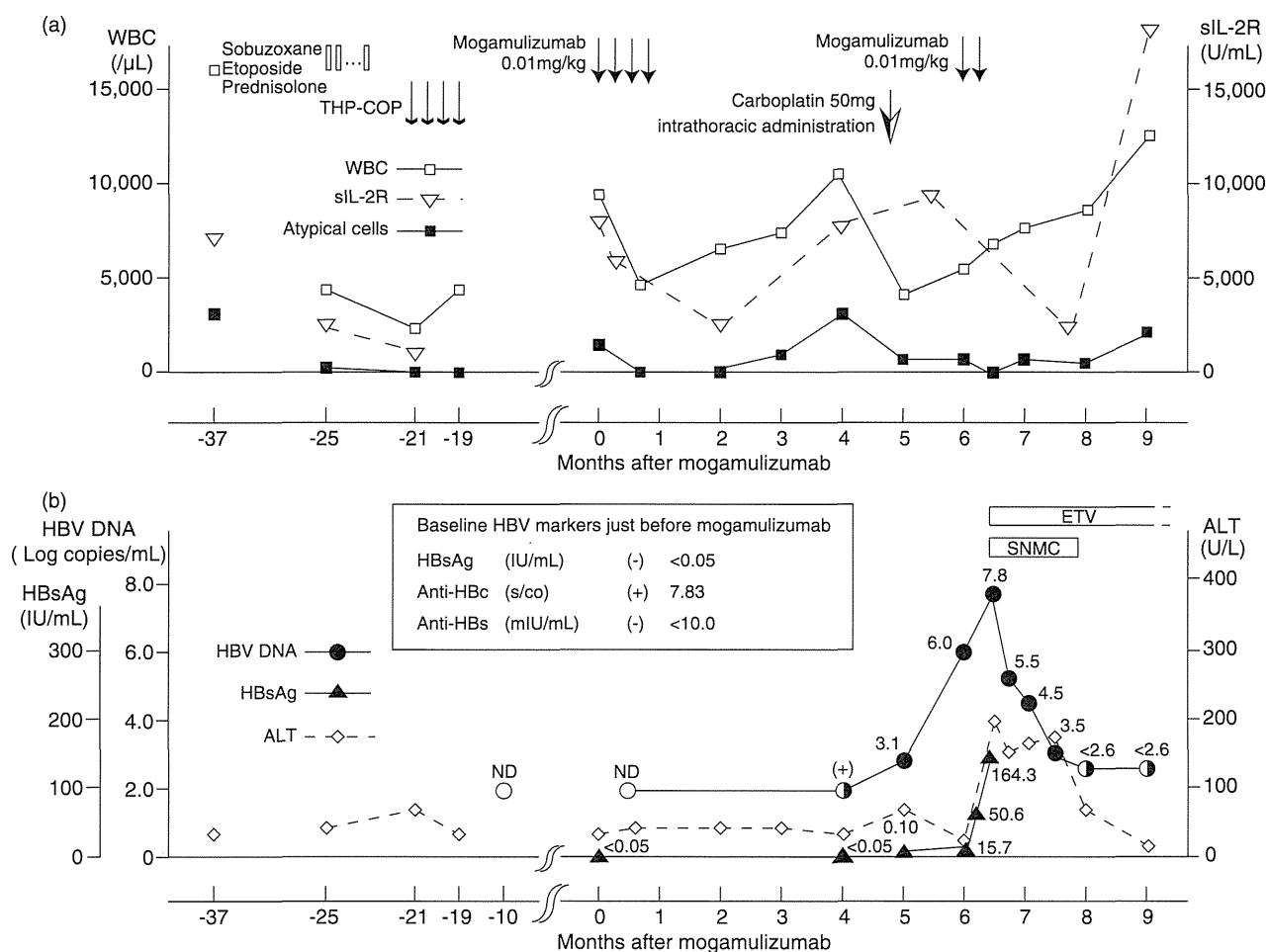


**Figure 1** Clinical course and kinetics of HBV markers in a patient with adult T-cell leukemia-lymphoma before and after the anti-CC chemokine receptor 4 monoclonal antibody mogamulizumab treatment. ALT, alanine aminotransferase; anti-HBc, antibody against hepatitis core antigen; anti-HBs, antibody against hepatitis surface antigen; ETV, entecavir; HBsAg, hepatitis B surface antigen; HBV, hepatitis B virus; ND, not detectable; sIL-2R, soluble interleukin-2 receptor; SNMC, Stronger Neo-Minophagen C; THP-COP, cyclophosphamide, pirarubicin, vincristine and prednisolone; WBC, white blood cells.



and an elevated lactate dehydrogenase value in peripheral blood in March 2007. She was enrolled into a phase 1 study for dose-finding of the anti-CCR4 antibody, mogamulizumab,<sup>9</sup> and received this antibody at 0.01 mg/kg by i.v. infusion once a week for 4 weeks (Fig. 1a, thin arrows). No combination of other anticancer chemotherapy was performed and no steroids were given, except for allergic prophylaxis. She was HBsAg negative at baseline on enrollment in the phase 1 study. Retrospective analysis using preserved samples revealed that she was anti-hepatitis B core positive, anti-hepatitis B surface negative, and HBV DNA was undetectable at baseline, attributed to previously resolved HBV infection (Fig. 1b). After mogamulizumab, ATL cells disappeared immediately from the peripheral blood, the nodal disease partially improved and no severe adverse event was observed. However, at 9 weeks after the end of mogamulizumab, the ATL cells reappeared in the peripheral blood. Furthermore, she received intrathoracic administration of carboplatin for involvement of ATL (right pleural effusion) in August 2007. During the next month, her cervical lymph nodes enlarged rapidly and we decided to re-treat with mogamulizumab because of the previous efficacy and safety of this antibody. After two doses of mogamulizumab, she was hospitalized in emergency due to ALT flare on October 2007 (Fig. 1b, 6.5 months after mogamulizumab). The laboratory findings showed that HBsAg had become positive and her HBV DNA levels increased to 7.8 log copies/mL, suggesting that the liver damage was caused by HBV reactivation. Entecavir (0.5 mg/day) and Stronger Neo-Minophagen C (40 mg/day) were given immediately and hepatitis B improved gradually (with ALT peaking at 205 U/L) for approximately 2 months. Entecavir was effective in controlling hepatitis B, and was continued for 1.5 years without any severe adverse events.

## DISCUSSION

THE PRESENTED CASE is the first report of HBV reactivation in a HBsAg negative patient receiving mogamulizumab. We analyzed preserved samples retrospectively and showed that her liver damage was attributable to HBV reactivation. Also, those analyses showed the following important findings regarding the kinetics of HBV DNA during reactivation: First, HBV DNA was undetectable at baseline, before administration of mogamulizumab. Elevated HBV DNA levels were detectable, in which polymerase chain reaction (PCR) signals were only detected 10 weeks prior to the development

of hepatitis and 13 weeks after the end of this antibody treatment. HBV DNA levels, measured by PCR-based assay, increased rapidly from 3.1 to 6.0 log copies/mL for 1 month and, finally, up to 7.8 log copies/mL. Second, the elevated HBV DNA levels preceded the detection of HBsAg (Architect Assay; Abbott Laboratories, North Chicago, IL, USA) by 1 month. Third, the patient was infected with HBV genotype C with a point mutation in the precore regions (G1896A) which might have been associated with the rapidly increasing kinetics of HBV DNA levels in this case.

How was the anti-CCR4 antibody mogamulizumab involved in the HBV reactivation? CCR4 is a chemokine receptor expressed on T-helper type 2 and regulatory T cells, and is thought to carry an important role in maintaining the balance of the human immune system.<sup>7-9</sup> It is difficult to demonstrate how mogamulizumab caused HBV reactivation in this case; the reduction of CCR4-expressing cells following this antibody treatment might have been associated with imbalance of antiviral immunity, resulting in the development of hepatitis due to HBV reactivation. Other than mogamulizumab, the intrathoracic administration of carboplatin and the ATL disease progression are considered to be factors potentially influencing HBV reactivation. However, retrospective analysis showed that HBV DNA levels were detectable in the peripheral blood before administration of carboplatin, suggesting that carboplatin is unlikely to have been mainly involved in the HBV reactivation. ATL is often diagnosed with a compromised immune system, and the disease progression might have been associated with reactivation of the virus. Interestingly, the timing of the rapid increase in ATL cells in the peripheral blood coincided with that of HBV replication in this case. However, disease progression of ATL alone is very unlikely to have caused the HBV reactivation because reactivation did not occur during the previous ATL progression.

To prevent hepatitis due to HBV reactivation, what lesson can we learn from this case? HBV reactivation following immunosuppressive therapy may lead to acute liver failure or fulminant hepatitis, and the patients have poor prognosis regardless of intensive antiviral treatment.<sup>11,12</sup> For preventing HBV reactivation in patients with previously resolved HBV infection, monitoring of HBV DNA-guided preemptive antiviral therapy is recommended in some guidelines,<sup>13,14</sup> however, the evidence of optimal interval of HBV DNA monitoring is limited. Most recently, monthly monitoring of HBV DNA was shown to effectively prevent HBV reactivation in patients with previously resolved HBV

infection who received rituximab plus steroids containing chemotherapy.<sup>15</sup> The kinetics of HBV reactivation in this case strongly suggested that monthly monitoring of HBV DNA could prevent hepatitis even in such a highly replicative clone with a precore mutation.

In summary, we first reported HBV reactivation following treatment with the anti-CCR4 antibody mogamulizumab and revealed the detailed kinetics of HBV replication during reactivation. Further well-designed studies are warranted to address the mechanisms of HBV reactivation and to establish standard management for reactivation in patients with previously resolved HBV infection, following anticancer chemotherapy and immunosuppressive therapy.

## ACKNOWLEDGMENTS

THIS STUDY WAS supported in part by the Ministry of Health, Labour and Welfare of Japan (Grant-in-Aid H24-kanen-004 to M. M.) and the Ministry of Education, Culture, Sports Science and Technology of Japan (Grant-in-Aid for Scientific Research (C) no. 90423855 to S. K.) and Grant-in-Aid for National Cancer Center Research and Development Fund (no. 23-A-17 to T. I.).

## REFERENCES

- 1 Lok AS, Liang RH, Chiu EK *et al.* Reactivation of hepatitis B virus replication in patients receiving cytotoxic therapy. Report of a prospective study. *Gastroenterology* 1991; **100**: 182–8.
- 2 Dervite I, Hober D, Morel P. Acute hepatitis B in a patient with antibodies to hepatitis B surface antigen who was receiving rituximab. *N Engl J Med* 2001; **344**: 68–9.
- 3 Hui CK, Cheung WW, Zhang HY *et al.* Kinetics and risk of de novo hepatitis B infection in HBsAg-negative patients undergoing cytotoxic chemotherapy. *Gastroenterology* 2006; **131**: 59–68.
- 4 Yeo W, Chan TC, Leung NW *et al.* Hepatitis B virus reactivation in lymphoma patients with prior resolved hepatitis B undergoing anticancer therapy with or without rituximab. *J Clin Oncol* 2009; **27**: 605–11.
- 5 Kusumoto S, Tanaka Y, Mizokami M *et al.* Reactivation of hepatitis B virus following systemic chemotherapy for malignant lymphoma. *Int J Hematol* 2009; **90**: 13–23.
- 6 Matsue K, Kimura S, Takanashi Y *et al.* Reactivation of hepatitis B virus after rituximab-containing treatment in patients with CD20-positive B-cell lymphoma. *Cancer* 2010; **116**: 4769–76.
- 7 Ishida T, Ueda R. Antibody therapy for Adult T-cell leukemia-lymphoma. *Int J Hematol* 2011; **94**: 443–52.
- 8 Ishii T, Ishida T, Utsunomiya A *et al.* Defucosylated humanized anti-CCR4 monoclonal antibody KW-0761 as a novel immunotherapeutic agent for adult T-cell leukemia/lymphoma. *Clin Cancer Res* 2010; **16**: 1520–31.
- 9 Yamamoto K, Utsunomiya A, Tobinai K *et al.* Phase I study of KW-0761, a defucosylated humanized anti-CCR4 antibody, in relapsed patients with adult T-cell leukemia-lymphoma and peripheral T-cell lymphoma. *J Clin Oncol* 2010; **28**: 1591–8.
- 10 Ishida T, Joh T, Uike N *et al.* Defucosylated anti-CCR4 monoclonal antibody (KW-0761) for relapsed adult T-cell leukemia-lymphoma: a multicenter phase II study. *J Clin Oncol* 2012; **30**: 837–42.
- 11 Sugawara K, Nakayama N, Mochida S. Acute liver failure in Japan: definition, classification, and prediction of the outcome. *J Gastroenterol* 2012; **47**: 849–61.
- 12 Oketani M, Ido A, Nakayama N *et al.* Etiology and prognosis of fulminant hepatitis and late-onset hepatic failure in Japan: summary of the annual nationwide survey between 2004 and 2009. *Hepato Res* 2013; **43**: 97–105.
- 13 Oketani M, Ido A, Uto H *et al.* Prevention of hepatitis B virus reactivation in patients receiving immunosuppressive therapy or chemotherapy. *Hepato Res* 2012; **42**: 627–36.
- 14 European Association For The Study Of The Liver. EASL clinical practice guidelines: management of chronic hepatitis B virus infection. *J Hepatol* 2012; **57**: 167–85.
- 15 Kusumoto S, Tanaka Y, Suzuki R *et al.* Prospective nationwide observational study of hepatitis B virus (HBV) DNA monitoring and preemptive antiviral therapy for HBV reactivation in patients with B-cell non-Hodgkin lymphoma following rituximab containing chemotherapy: results of interim analysis. *Blood* 2012; **120**: abstract 2641.

# Induction of CD8 T-cell responses restricted to multiple HLA class I alleles in a cancer patient by immunization with a 20-mer NY-ESO-1f (NY-ESO-1 91-110) peptide

Shingo Eikawa<sup>1,2</sup>, Kazuhiro Kakimi<sup>3</sup>, Midori Isobe<sup>2</sup>, Kiyotaka Kuzushima<sup>4</sup>, Immanuel Luescher<sup>5</sup>, Yoshihiro Ohue<sup>2</sup>, Kazuhiro Ikeuchi<sup>1</sup>, Akiko Uenaka<sup>6</sup>, Hiroyoshi Nishikawa<sup>7</sup>, Heiichiro Udono<sup>1</sup>, Mikio Oka<sup>2</sup> and Eiichi Nakayama<sup>6</sup>

<sup>1</sup> Department of Immunology, Okayama University Graduate School of Medicine, Dentistry and Pharmaceutical Sciences, Okayama, Japan

<sup>2</sup> Department of Respiratory Medicine, Kawasaki Medical School, Kurashiki, Japan

<sup>3</sup> Department of Immunotherapeutics, University of Tokyo Hospital, Tokyo, Japan

<sup>4</sup> Department of Immunology, Aichi Cancer Center, Nagoya, Japan

<sup>5</sup> Ludwig Institute for Cancer Research, University of Lausanne, Epalinges, Switzerland

<sup>6</sup> Faculty of Health and Welfare, Kawasaki University of Medical Welfare, Kurashiki, Japan

<sup>7</sup> Department of Experimental Immunology, Immunology Frontier Research Center, Osaka University, Osaka, Japan

Immunogenicity of a long 20-mer NY-ESO-1f peptide vaccine was evaluated in a lung cancer patient TK-f01, immunized with the peptide with Picibanil OK-432 and Montanide ISA-51. We showed that internalization of the peptide was necessary to present CD8 T-cell epitopes on APC, contrasting with the direct presentation of the short epitope. CD8 T-cell responses restricted to all five HLA class I alleles were induced in the patient after the peptide vaccination. Clonal analysis showed that B\*35:01 and B\*52:01-restricted CD8 T-cell responses were the two dominant responses. The minimal epitopes recognized by A\*24:02, B\*35:01, B\*52:01 and C\*12:02-restricted CD8 T-cell clones were defined and peptide/HLA tetramers were produced. NY-ESO-1 91-101 on A\*24:02, NY-ESO-1 92-102 on B\*35:01, NY-ESO-1 96-104 on B\*52:01 and NY-ESO-1 96-104 on C\*12:02 were new epitopes first defined in this study. Identification of the A\*24:02 epitope is highly relevant for studying the Japanese population because of its high expression frequency (60%). High affinity CD8 T-cells recognizing tumor cells naturally expressing the epitopes and matched HLA were induced at a significant level. The findings suggest the usefulness of a long 20-mer NY-ESO-1f peptide harboring multiple CD8 T-cell epitopes as an NY-ESO-1 vaccine. Characterization of CD8 T-cell responses in immunomonitoring using peptide/HLA tetramers revealed that multiple CD8 T-cell responses comprised the dominant response.

The NY-ESO-1 antigen was originally identified in esophageal cancer by serological expression cloning (SEREX) using autologous patient serum.<sup>1,2</sup> NY-ESO-1 expression is observed in a

**Key words:** cancer vaccine, NY-ESO-1, long peptide, CD8 T-cell response

Additional Supporting Information may be found in the online version of this article.

This article was published online on 22 June 2012. An error was subsequently identified. This notice is included in the online and print versions to indicate that both have been corrected 21 November 2012.

**Grant sponsor:** Ministry of Education, Culture, Sports, Science and Technology of Japan (Grant-in-Aid for Scientific Research (B)), New Energy and Industrial Technology Development Organization (NEDO), Japan

**DOI:** 10.1002/ijc.27682

**History:** Received 11 Jan 2012; Accepted 1 Jun 2012; Online 22 Jun 2012

**Correspondence to:** Eiichi Nakayama, M.D., Faculty of Health and Welfare, Kawasaki University of Medical Welfare, 288 Matsushima, Kurashiki, Okayama 701-0193, Japan, Tel.: +81-86-462-1111 ext. 54954, Fax: +81-86-464-1109, E-mail: nakayama@mw.kawasaki-m.ac.jp

wide range of human malignancies, but the expression is restricted to germ cells in the testes in normal adult tissues.<sup>1-4</sup> Therefore, NY-ESO-1 has emerged as a prototype of a class of cancer/testis (CT) antigens.<sup>5</sup> The efficacy of the NY-ESO-1 antigen as a cancer vaccine has been studied extensively using various preparations, *e.g.*, peptide, protein or DNA, etc. of the antigen with various adjuvants.<sup>6-14</sup> These studies established the safety of the NY-ESO-1 vaccine and demonstrated its immunogenicity.

In a phase I clinical trial, we immunized cancer patients with a complex of cholesterol-bearing hydrophobized pullulan and NY-ESO-1 whole protein (CHP-NY-ESO-1) and showed that the vaccine had potent capacity to induce the NY-ESO-1 antibody in vaccinated patients.<sup>13,14</sup> The most dominant serological antigenic epitope was NY-ESO-1 91-108. The CHP-NY-ESO-1 vaccine also elicited CD4 and CD8 T-cell responses in immunized patients.<sup>14</sup> Analysis of T cell responses against overlapping peptides (OLPs) spanning the NY-ESO-1 molecule revealed that two dominant NY-ESO-1 regions, regions II (73-114) and III (121-144), were recognized by either CD4 or CD8 T-cells in most patients irrespective of their HLA type. Essentially similar findings were obtained by studies using other preparations of NY-ESO-1 protein vaccine.<sup>11,12,15</sup>

**What's new?**

An antigen called NY-ESO-1 is expressed by a wide range of human cancers, and has shown promise as a cancer vaccine. In this study, the authors studied a peptide derived from that antigen, and analyzed the cellular and molecular mechanisms that allow the peptide to provoke an immune response. They found that the peptide must be internalized by antigen-presenting cells (APCs) in order to yield T-cells that can attack tumours via the NY-ESO-1 antigen. These data increase our understanding of the requirements for an effective therapeutic cancer vaccine. (This section added after initial online publication.)

CD8 T-cells induced by immunization with NY-ESO-1 class I short epitope peptides have been shown to be of low affinity and do not recognize naturally processed NY-ESO-1 on tumor cells.<sup>16</sup> However, the advantage of synthetic long peptides over short peptides for use as vaccines has been reported.<sup>17</sup> Long peptides do not bind to MHC class I molecules directly, and require antigen processing by dendritic cells to be presented. Therefore, the use of long peptides prevents the antigen peptides from direct binding to MHC class I molecules on nonprofessional antigen-presenting cells (APC), which may cause transient activation and subsequent anergy of CTLs in the absence of appropriate costimulatory signals.<sup>17-19</sup> Based on these findings, we recently used a long peptide spanning a peptide region NY-ESO-1 91-110 (NY-ESO-1f peptide) which included the dominant serological antigenic epitope and overlapped one of the two dominant regions recognized by CD4 and CD8 T-cells for a vaccine in a clinical trial.<sup>20</sup> Ten patients received the NY-ESO-1f peptide vaccine. The NY-ESO-1f peptide vaccine was well tolerated and elicited humoral, CD4 and CD8 T-cell responses in immunized patients.

In this study, we demonstrated that internalization of the peptide was necessary to present CD8 T-cell epitopes on APC treated with the long 20-mer NY-ESO-1f peptide. Analysis of the CD8 T-cell response in an NY-ESO-1f peptide-immunized patient revealed occurrence of responses restricted to all five HLA class I alleles defined in the patient. The frequency of A\*24:02, B\*35:01, B\*52:01, C\*03:03 and C\*12:02-restricted CD8 T-cells in PBMCs was defined by clonal analysis revealing B\*35:01- and B\*52:01-restricted CD8 T-cell responses as dominant. By establishing clones from those HLA-restricted CD8 T-cells, new epitopes on A\*24:02, B\*35:01, B\*52:01 and C\*12:02 were defined and peptide/HLA tetramers were prepared. Clonal analysis showed that CD8 T-cells that recognize natural epitopes on tumor cells were induced in a significant proportion by immunization with the NY-ESO-1f peptide. Immunomonitoring using the tetramers revealed that multiple CD8 T-cell responses comprised the dominant response.

**Material and Methods****Clinical trial**

A phase I clinical trial of the NY-ESO-1f peptide vaccine was conducted to evaluate the safety, immune response and tumor response.<sup>20</sup> Patients with advanced cancers that were refractory to standard therapy and expressed NY-ESO-1 as assessed by immunohistochemistry (IHC) were eligible. The protocol was approved by the Ethics Committee of Tokyo,

Osaka and Okayama Universities in light of the Declaration of Helsinki. Written informed consent was obtained from each patient before enrolling in the study. The study was performed in compliance with Good Clinical Practice. The study was registered in the University hospital Medical Information Network Clinical Trials Registry (UMIN-CTR) Clinical Trial (Unique trial number: UMIN00001260) on July 24, 2008 (UMIN-CTRURL: <http://www.umin.ac.jp/ctr/index.htm>).

**Blood samples**

Patient TK-f01 was a lung cancer patient who received a right middle lobectomy in October, 2004.<sup>20</sup> As the tumor continued to grow despite chemotherapy, he was enrolled in the study in June, 2008. The patient received 12 vaccinations once every 3 weeks. Peripheral blood was drawn from patient TK-f01 with informed consent for immunological monitoring. Peripheral blood mononuclear cells (PBMCs) were isolated from heparinized blood by density gradient centrifugation using a Histopaque 1077 (Sigma-Aldrich, St. Louis, MO). CD4-, CD8- and CD19-positive cells were purified by magnetic cell sorting (Miltenyi Biotec, Bergisch Gladbach, Germany). The residual cells were kept for use as APC. The cells were stored in liquid N<sub>2</sub> until use. HLA typing was done with PBMCs by a sequence-specific oligonucleotide probe and sequence-specific priming of genomic cDNA using a standard procedure.

**Cell lines**

LC99A and OU-LC-OK are lung cancer cell lines. SK-OV3 is an ovarian cancer cell line and SK-MEL37 is a melanoma cell line. These cell lines were kept by serial passage in tissue culture. EBV-B cells were generated from CD19-positive peripheral blood B cells using a culture supernatant from EBV-producing B95-8 cells. The medium used to maintain these cell lines was RPMI1640 supplemented with 10% FCS (JRM, Bioscience, Lenexa, KA), 2 mmol/l Glutamax, antibiotics, and 10 mmol/l HEPES (Invitrogen, Carlsbad, CA).

**Antibodies**

Anti-human CD4, anti-human CD8, anti-HLA class I and anti-HLA class II mAbs were purchased from BD Bioscience (San Jose, CA).

**Peptides**

The following series of 28 18-mer OLPs and a C-terminal 30-mer peptide spanning the entire NY-ESO-1 protein were used: 18.1 (1-18), 18.2 (7-24), 18.3 (13-30), 18.4 (19-36), 18.5 (25-42), 18.6 (31-48), 18.7 (37-54), 18.8 (43-60), 18.9 (49-

66), 18.10 (55-72), 18.11 (61-78), 18.12 (67-84), 18.13 (73-90), 18.14 (79-96), 18.15 (85-102), 18.16 (91-108), 18.17 (97-114), 18.18 (103-120), 18.19 (109-126), 18.20 (115-132), 18.21 (121-138), 18.22 (127-144), 18.23 (133-150), 18.24 (139-156), 18.25 (145-162), 18.26 (149-166), 18.27 (153-170), 18.28 (156-173) and 30.9 (151-180). Various N- and C-termini truncated peptides in the NY-ESO-1f peptide were also used. These peptides were synthesized using standard solid-phase methods based on *N*-(9-fluorenyl)-methoxycarbonyl (Fmoc) chemistry on an ABIMED Multiple Peptide Synthesizer (AMS422, ABIMED, Langenfeld, Germany) at Okayama University (Okayama, Japan). The carboxyfluorescein (FAM)-conjugated NY-ESO-1f peptide (5(6)-FAM-YLAMPFATPMEAE-LARRSLA) was synthesized by Operon (Tokyo, Japan).

### Recombinant NY-ESO-1 protein

Recombinant NY-ESO-1 protein was prepared as described earlier.<sup>13</sup> NY-ESO-1 cDNA was cloned into the *SphI/SalI* and *BamHI/SphI* sites of the pQE-30 vector. N-His tagged protein was purified by nickel-ion affinity chromatography under denaturing conditions.

### Preparation of immature dendritic cells

Monocytes were isolated from PBMCs using anti-CD14 mAb-coated magnetic beads (Miltenyi Biotec) and cultured in AIM-V medium supplemented with 5% heat-inactivated pooled human serum, 10 ng/ml rhGM-CSF (Kyowa Hakko Kirin, Tokyo, Japan) and 10 ng/ml rhIL-4 (PeproTech) for 7 days at 37°C in a 5% CO<sub>2</sub> atmosphere.

### *In vitro* stimulation of bulk CD4 and CD8 T-cells

CD4 and CD8 T-cells ( $2 \times 10^6$ /well) were cultured with a mixture of 29 NY-ESO-1 OLPs ( $10^{-6}$  M) in the presence of an equal number of irradiated (40 Gy), autologous CD4- and CD8-depleted cells as APC in a 24-well culture plate (BD Bioscience) for 12 days at 37°C in a 5% CO<sub>2</sub> atmosphere. The medium was AIM-V (Invitrogen) supplemented with 5% heat-inactivated pooled human serum, 2 mM L-glutamine, 100 IU/ml penicillin, 100 µg/ml streptomycin, 10 units/ml recombinant human (rh) IL-2 (Takeda Chemical Industries, Osaka, Japan) and 10 ng/ml rhIL-7 (PeproTech, London, UK).

### Cloning of CD8 T-cells

CD8 T-cells were cloned by limiting dilution after *in vitro* stimulation in round-bottomed 96-well plates in the presence of irradiated (40 Gy) allogeneic PBMCs freshly prepared from the healthy donor as feeder cells. The medium used was AIM-V (Invitrogen) supplemented with 5% heat-inactivated pooled human serum, 2 mM L-glutamine, 100 IU/ml penicillin, 100 µg/ml streptomycin, 20 units/ml rhIL-2 (Takeda Chemical Industries), 10 ng/ml rhIL-7 (PeproTech) and 1 µg/ml phytohemagglutinin (PHA)-L (Sigma-Aldrich).

### Clonal expansion

Cloned CD8 T-cells ( $1 \times 10^3$ ) obtained by limiting dilution were expanded in a round-bottomed 96 well plate in the

presence of irradiated (40 Gy) PBMCs ( $5 \times 10^4$ ) freshly prepared from allogeneic healthy donors as feeder cells. Fresh medium was added every 3 days. After culture for 14 days, the cells were harvested and kept frozen at  $2 \times 10^6$ /tube. The medium used was AIM-V supplemented with 5% heat-inactivated pooled human serum, 2 mM L-glutamine, 100 IU/ml penicillin, 100 µg/ml streptomycin, 20 units/ml rhIL-2, 10 ng/ml rhIL-7 and 1 µg/ml phytohemagglutinin (PHA)-L.

### IFN $\gamma$ capture assay

Bulk CD4 or CD8 T-cells ( $1 \times 10^5$ ) from the *in vitro* stimulation culture were cultured with autologous or allogeneic EBV-B cells ( $1 \times 10^5$ ) pulsed with OLPs for 4 hr. The cells were then treated with a bi-specific CD45 and IFN $\gamma$  antibody (IFN $\gamma$  catch reagent) (2 µl) for 5 min on ice. The cells were diluted in AIM-V medium (3 ml) and placed on a slow rotating device (Miltenyi Biotec) to allow IFN $\gamma$  secretion at 37°C in a 5% CO<sub>2</sub> atmosphere. After incubation for 45 min, the cells were washed with cold buffer and treated with PE-conjugated anti-IFN $\gamma$  (detection reagent), and FITC-conjugated anti-CD4 or anti-CD8 mAb. After incubation for 10 min at 4°C, the cells were washed and analyzed by a FACS Canto II (BD Bioscience).

### Tetramer construction and staining

Peptide/HLA tetramers were produced as described earlier.<sup>21,22</sup> NY-ESO-1 91-101/A\*24:02, NY-ESO-1 92-100/B\*35:01, NY-ESO-1 92-102/B\*35:01, NY-ESO-1 94-104/B\*35:01 and NY-ESO-1 96-106/C\*12:02 tetramers were used. The HIV Env/A\*24:02 tetramer was used as a control. For staining, cells were incubated with tetramer at a concentration of 20 µg/ml for 15 min at 37°C, followed by incubation with an FITC-conjugated anti-CD8 mAb (Miltenyi Biotec) on ice for 15 min and analyzed by a FACS Canto II (Becton Dickinson).

### Cytotoxicity assay

Cytotoxicity was assayed by a luminescent method using the aCella-Tox kit (Cell Technology, Mountain View, CA). Effector cells were incubated with 5,000 target cells at various ratios in 96-well round bottomed culture plates for 12 hr at 37°C in a 5% CO<sub>2</sub> atmosphere. The plate was read by a luminometer (multi-detection microplate reader, DS Pharma, Osaka, Japan).

### IFN $\gamma$ ELISA

CD8 T-cell clones ( $5 \times 10^3$ ) were cultured with autologous or allogeneic EBV-B cells ( $5 \times 10^3$ ) pulsed with the peptides in a 96-well round bottomed culture plate for 24 hr at 37°C in a 5% CO<sub>2</sub> atmosphere. Culture supernatants were then collected and the amount of IFN $\gamma$  was measured by sandwich ELISA. For antibody blocking experiments, each mAb (5 µg/ml) was added to the assay culture. To inhibit internalization of the antigens to DCs, cytochalasin B (10 µM) was added to the culture.

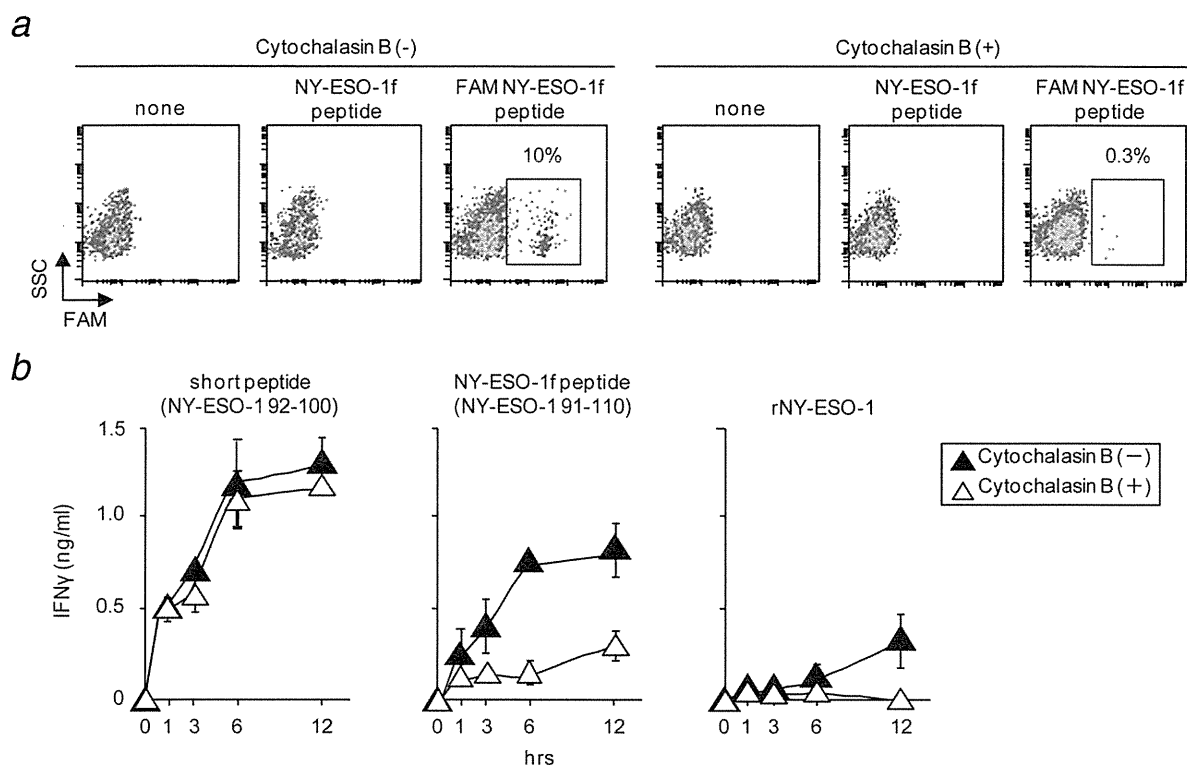


Figure 1. Internalization and processing of the long 20-mer NY-ESO-1f-peptide by APC in CD8 T-cell recognition. In (a), immature dendritic cells (iDCs) from a healthy donor (HD) NO PBMCs (A\*02:07/\*26:02, B\*35:01/\*46:01, C\*08:03/\*14:03) were cultured with an NY-ESO-1f peptide (10  $\mu$ M) or a FAM NY-ESO-1f peptide (10  $\mu$ M) for 12 hr in the presence or absence of cytochalasin B (10  $\mu$ M). After culture, the internalization of the FAM NY-ESO-1f peptide was analyzed by FACS Canto II. In (b), the CD8 T-cell clone 2H10 ( $5 \times 10^3$ ) was stimulated with iDCs ( $5 \times 10^3$ ) pulsed with the short peptide (NY-ESO-1 92-100: LAMPFATPM, 9-mer; 1  $\mu$ M), the NY-ESO-1f peptide (NY-ESO-1 91-110: YLAMPFATPMEAE LARRSLA, 20-mer; 1  $\mu$ M) or recombinant NY-ESO-1 protein (1  $\mu$ M) for the indicated time in the presence or absence of cytochalasin B (10  $\mu$ M). The amount of IFN $\gamma$  in the culture supernatant was determined by ELISA. One representative of three independent experiments is shown.

## Results

### Internalization of 20-mer NY-ESO-1f peptide to present CD8 T-cell epitopes on antigen presenting cells

We investigated the need for internalization of the 20-mer NY-ESO-1f peptide (NY-ESO-1 91-110: YLAMPFATPMEAE LARRSLA) to present CD8 T-cell epitopes on APC. Immature dendritic cells (iDCs) were prepared from purified CD14-positive cells from a B\*35:01 healthy donor by treating them with IL-4 and GM-CSF for 7 days and used as APC. As shown in Figure 1a, internalization of the FAM-conjugated NY-ESO-1f peptide was observed in approximately 10% of DCs after culture with the peptide for 12 hr. Treatment of DCs with the peptide in the presence of cytochalasin B diminished internalization. Recognition by a B\*35:01-restricted CD8 T-cell clone 2H10 of DCs treated with the peptides was investigated. As shown in Figure 1b, clone 2H10 recognized DCs pulsed with the short peptide NY-ESO-1 92-100 in the presence of cytochalasin B. On the other hand, recognition of DCs pulsed with NY-ESO-1f peptide was inhibited in the presence of cytochalasin B. Only marginal recognition was observed with DCs pulsed with recombinant NY-ESO-1 protein.

### Multiple HLA class I-restricted CD8 T-cell responses in PBMCs from patient TK-f01 immunized with the 20-mer NY-ESO-1f peptide

TK-f01 was a lung adenocarcinoma patient immunized with the NY-ESO-1f peptide (600  $\mu$ g) with Picibanil OK-432 and Montanide ISA-51 12 times once every 3 weeks.<sup>20</sup> We investigated multiple HLA class I-restricted CD8 T-cell responses in PBMCs from patient TK-f01. The patient's HLA class I was A\*24:02, B\*35:01, B\*52:01, C\*03:03 and C\*12:02. Purified CD8 T-cells from the patient's PBMCs obtained at day 64 after the third vaccination were stimulated once with a mixture of 29 18-mer series of NY-ESO-1 OLPs spanning the entire protein for 12 days using CD4 and CD8-depleted PBMCs as APC. The cells were harvested and stimulated with NY-ESO-1f peptide for 4 hrs using autologous and allogeneic EBV-B cells as APC and the response was assayed by IFN $\gamma$  capture assay. As shown in Figure 2, TK-f01 CD8 T-cells responded strongly to NY-ESO-1f peptide-pulsed autologous EBV-B cells. Use of various allogeneic EBV-B cells as APC showed TK-f01 CD8 T-cell responses against NY-ESO-1f peptide presented on multiple HLA class I molecules shared with patient TK-f01.